Geometry of the Universe in Extreme Cosmology: The v=c=0 Paradox

Preprint available on Zenodo: https://doi.org/10.5281/zenodo.16995736

Mikheili Mindiashvili
Independent Researcher
Former Lecturer at Kutaisi Technical University
mindia-m@mail.ru

***Objective**: To present a new geometric model for the analysis and visualization of relativistic effects, including velocity addition, gravitational phenomena, and extreme states of matter.*
***Methods**: A step-by-step analytical approach using simple geometry is employed, allowing complex concepts to be gradually understood. The method combines kinematic and gravitational interpretations. It is supported by mathematical justification and allows for experimental verification.*
***Results**: It is shown that the fundamental equality $v=c=0$ arises as a consequence of the symmetric structure of spacetime. The method is consistent with relativistic formulas and enables clear computations and geometric interpretations.*
***Conclusions**: The step-by-step presentation ensures transparency of verification, reproducibility of results, and opens new possibilities for interpreting extreme states of matter and for practical applications of the model.*

Keywords: special relativity, relativistic geometry, mirror-symmetric geometry, singularity, Schwarzschild radius, time dilation, infinity, phase transition, critical state v=c=0, angle φ, extreme matter states.

1. Introduction

The study of the fundamental properties of space and time remains one of the central challenges of modern physics. Despite significant advances in relativity theory and cosmology, a number of questions concerning the behavior of physical quantities near singular states have yet to receive definitive answers. In particular, the description of the initial conditions of the Universe's evolution remains under discussion. The interpretation of the singularity at T = 0 is also a subject of active theoretical debate.

In this work, a hypothetical model of the Universe's geometry is proposed. It is based on simple geometric constructions combined with the principles of relativistic velocity addition and mirror symmetry. From the very beginning, a new tool—the angle φ—is introduced, which later proves to be crucial in this geometry for understanding relativistic and gravitational effects. Its application allows the revelation of potentially unexpected patterns and helps to avoid numerical and conceptual "dead ends" characteristic of extreme states of physical quantities.

Within the framework of the proposed model, an analysis of the behavior of physical quantities at the moment T = 0 — corresponding to the so-called singularity—has been conducted. However, in this geometry, a "mild" singularity emerges, concentrated at the Schwarzschild radius.

A key aspect of the study is the mirror-symmetric calculation method (the φ-method). It allows "problematic" angles to be replaced with complementary ones, separating formulas into sine and cosine branches. This enhances computational stability and makes the behavior of functions at boundaries both transparent and predictable. Preliminary investigations have shown encouraging results: chaotic graphs are transformed into smooth, easily interpretable forms, and numerical procedures remain stable even near critical values. Moreover, this method opens additional possibilities for analyzing complex relativistic equations and the behavior of matter under extreme conditions. For instance, upon approaching the speed of light, the method produces an unexpected result: at the moment when $v = c$, the equality $v = c = 0$ emerges. At this instant, matter and antimatter may convert into each other through a special state of the metric.

This equality, $v=c=0$, is not a product of arbitrary imagination. It directly follows from relativistic velocity addition and is further verified in this study using alternative methods.

The introduction of the principle of mirror symmetry into the geometric description of relativistic effects provides a more harmonious understanding of known regularities. It also establishes a foundation for addressing several previously unresolved or complex problems. The φ-method ensures a stable description of processes near boundary conditions, including situations where traditional approaches lead to divergent solutions. Thus, the proposed tool may not only hold theoretical value but also possess potential practical applications in computational algorithms, enabling the automatic verification of calculation stability under extreme conditions.

The most remarkable aspect of the proposed model is its ability to "trace" the trajectories of

matter and antimatter in extreme states. Matter with a symmetric structure can formally reach the speed of light, simultaneously transitioning into a new state where v=c=0. This effect opens the prospect of modeling processes traditionally considered unreachable. These include the behavior of particles near singularities and the evolution of the Universe at moments approaching T=0.

Thus, the proposed geometric model provides an intriguing foundation for further analysis. The gradual introduction of concepts allows one to progress from intuitive understanding to rigorous mathematical description. This approach stimulates new hypotheses regarding the interaction of matter and antimatter and the dynamics of gravitational and relativistic effects. It also suggests potential experiments with high-energy particles. The proposed model may find applications across various fields of science—from atomic and classical physics to astrophysics and string theory. It can be used to visualize the motion of planets, stars, and galaxies. It can also model black holes, providing an accurate, stable, and intuitive representation of physical processes. Even partial confirmation of its validity would open new prospects for further research in the modeling and digitization of the Universe, allowing a fresh perspective on fundamental laws.

2. Motivation – Problem Statement

Modern physics, particularly in the realm of general relativity (GR), is built upon complex mathematical constructs such as tensors, spacetime curvature, and Riemannian geometry [1, 2]. Despite their precision and predictive power, these methods often remain challenging to intuitively understand and visualize, especially outside the professional community [3, 4].

Through numerous thought experiments, a configuration of several geometric figures was identified that enabled the visualization of relativistic velocity addition in space. In certain extreme cases, this geometry revealed the unusual equality $v = c = 0$. Remarkably, the formulas of relativistic physics are consistent with this equality.

This discovery provided the foundation for studying this geometry not only from a kinematic perspective but also considering gravitational characteristics.

Given the existing challenges in traditional relativity theory, there is a need for a more intuitive yet substantive model capable of providing a new perspective on gravity and related phenomena. In this work, a geometric model is proposed, based on the angle φ formed in a right triangle. The hypotenuse of this triangle corresponds to the limiting velocity or the critical radius (e.g., the Schwarzschild radius) [5, 6]. This angle φ becomes a central quantity through which both gravitational curvature and relativistic effects—such as time dilation—can be expressed.

The model is simple in its construction but profound in its implications. It demonstrates that many physical effects can be reduced to the variation of a single parameter—the angle φ, which depends on the ratio of the current radius to the gravitational radius. This allows for the interpretation of processes at the boundary of a black hole and the study of extreme states of matter. It also enables the potential prediction of system behavior under extreme conditions [7, 8].

Moreover, through the angle φ, a hidden trigonometric structure becomes apparent. This structure is already present in the formulas of relativistic physics but was previously unused for analyzing extreme cases. This approach allows singularities (for example, $\gamma \to \infty$ or $\cos \varphi \to 0$)

to be visualized and bypassed, enabling the interpretation of extreme states and opening the way to new physical hypotheses.

Thus, the proposed approach can be regarded as an intuitive alternative to tensor-based descriptions, capable not only of interpreting known effects but also of serving as a source of new physical hypotheses.

3. Geometric Model of Spacetime Curvature via the Angle φ

This section provides a detailed description of the geometric construction of the proposed model, which is based on a right triangle reflecting the fundamental aspects of gravity and relativistic effects (see Figure 1) [1, 9].

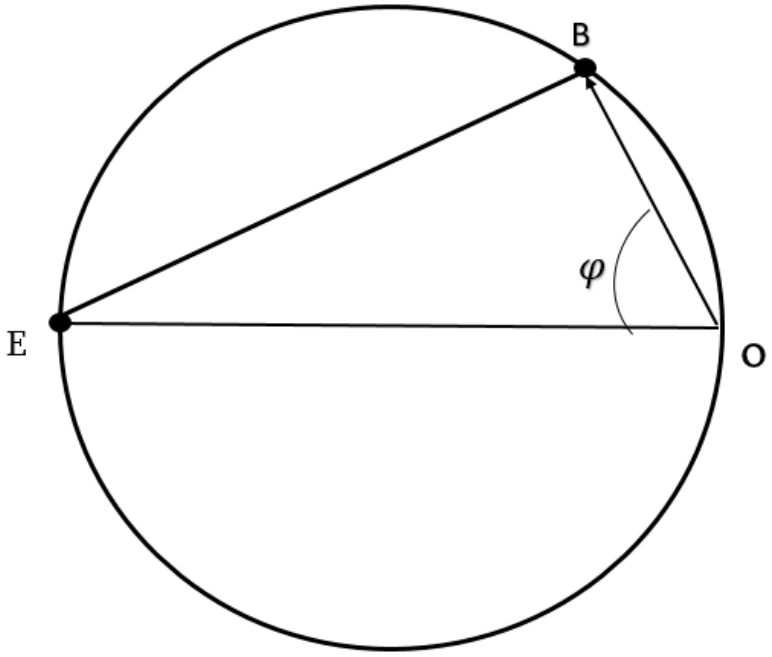

Figure 1 — *A rectangle inscribed in a circle*

1. Elements of the geometric scheme:

- Point O: the reference point or the center of a gravitational object, such as the Earth, the Sun, a black hole, or the Universe.
- Point B: the surface of the object, defining its physical radius r or velocity.
- Point E: a point on the hypotenuse corresponding to the maximum possible state (e.g., the limiting velocity or the maximum radius).

2. Interpretation of the triangle's sides:

- Leg OB: the physical radius of the object, r. The smaller this radius for a given mass, the stronger the gravitational effects. Additionally, leg OB can be used to visualize the velocity of the object depending on the problem at hand.
- Leg BE: represents, for example, relativistic distortions. It links the radius, velocity, and time dilation.

- Hypotenuse OE: the maximum possible value, such as the speed of light c or a critical radius.

3. The angle φ and its significance:

- The angle φ is located between leg OB and the hypotenuse OE.
- It can be expressed as: $\varphi = \arccos\left(\sqrt{1 - \frac{r_s}{r}}\right)$
- The closer the object is to, for example, the Schwarzschild radius, the larger φ becomes, approaching 90° [10].
- For large values of $r\ (r \gg r_s)$, the angle φ is small and approaches 0. In this case, spacetime is almost flat.

4. Physical interpretation of φ:

- The angle φ unifies parameters such as velocity, mass, radius, gravitational time dilation, and relativistic distortions.
- It is a universal parameter reflecting the overall degree of spacetime curvature and the associated relativistic effects.

5. Advantages of the model:

- Simple visualization.
- Applicable to any object—from planets and satellites to black holes.
- It can replace cumbersome tensor calculations in qualitative analyses of gravitational effects [11].

4. Geometric Interpretation of Relativistic Velocity Addition

Such a geometric arrangement offers several advantages. It provides a clear and intuitive visualization of many relativistic effects. This geometry can be adapted for various tasks, adjusting it to specific conditions. Therefore, before moving on to other sections of the article, it is useful to delve into its details.

Within the study of the geometric model of spacetime interactions, a unique concept has been proposed, based on the use of a relativistic triangle. This allows velocities and their interactions to be considered within a geometric framework. A key characteristic here is the diameter of the circle, which corresponds to the speed of light, c.

In this approach, each point on the surface of the circle or along the arc OE represents the state of motion of material objects. This makes it possible to relate the orbital parameters of objects to the geometric structure of spacetime.

Consider a circle (Figure 2) whose diameter corresponds to the speed of light, c. In this model, an additional projection of motion relative to an auxiliary point E is also provided.

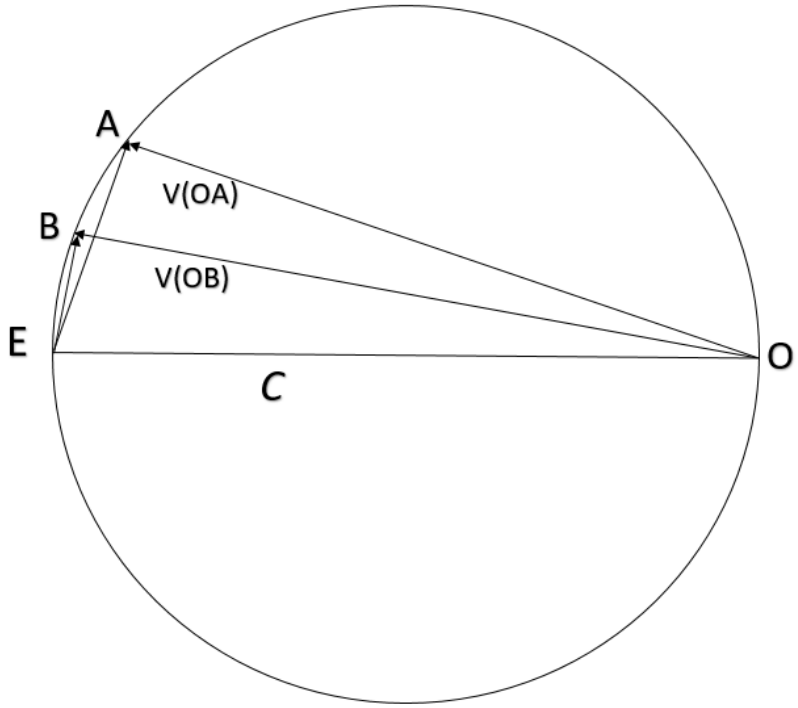

Figure 2 — *Geometric Interpretation of Relativistic Velocity Addition*

Let two points, A and B, be located on the arc. Each of them has its own velocity: $v(OA)$ and $v(OB)$, represented as the legs of the corresponding triangles. The geometric structure of the circle allows the relative velocity between points A and B to be expressed in a more accurate way. Instead of simple algebraic subtraction, the relativistic law of velocity addition is used [12]:

$$v(OB) = \frac{v(OA) + v(AB)}{1 + \frac{v(OA)v(AB)}{c^2}} \quad (1)$$

Visually, this operation corresponds to linking the triangles △OAE and △OEB through the common hypotenuse c. In this case, the legs of these triangles are not added directly but are subject to a constraint determined by their geometric relationship and the properties of spacetime.

The correspondence between the lengths of the legs and the hypotenuse with the relativistic velocity addition formula can be verified through appropriate calculations and using geometric tools.

Any triangle △OBE or △OAE inscribed in a circle such that its hypotenuse coincides with the diameter fully obeys the Pythagorean theorem and trigonometric relationships [13]. For simplifying the analysis in subsequent studies, it is convenient to consider the motion of the triangle vertices A and B along the arc OE, which allows tracking changes in the shapes and angles of the right triangles dynamically.

Regardless of the positions of points A and B on the arc, formula (1) remains valid, ensuring continuity and internal consistency of the calculations. This result holds even in extreme cases, when points A or B coincide with the initial point O or the terminal point E, confirming the universality and stability of the proposed model.

The primary aim of our study is to examine the behavior of points under extreme conditions. We also analyze which phases of the Universe's evolution correspond to these situations within the proposed geometric model. Naturally, this geometry can be visualized using computer graphics and an appropriate script; however, employing imagination for visualization enhances the perception and understanding of the results obtained. For this reason, in the following paragraphs, we will gradually adapt this geometry step by step, taking into account not only velocities but also gravitational quantities.

Thus, all points on the arc of the circle are connected not according to the classical rule of velocity addition, but in a relativistic manner. This approach automatically accounts for the speed limit c and ensures a consistent representation of relative motions within the finite geometric structure. The geometric model provides a clear visualization of how velocities, differing at various points, transform relative to each other by forming the corresponding triangle. All such triangles always share a common hypotenuse.

For each object moving at a certain velocity v, a right triangle can be associated, inscribed in a circle, in which the principle of relativistic velocity addition is preserved.

Moreover, the model shows that the connection between gravity and motion can be expressed not only through the traditional curvature of the metric but also through the difference in velocities between points within the geometric structure of the circle.

A confirmation of this geometric consistency is the fact that for any two points A and B within such a geometric space, one can find a third point E and a fourth symmetrically located point O (or vice versa, see Figure 2), relative to which the relativistic velocity addition formula operates correctly. This confirms that the proposed geometry is not only compatible with relativistic principles but also strictly adheres to them.

For a clear visualization, consider the following example:

At the initial moment T_0, three points—O, A, and B—begin to move symmetrically away from each other along a straight line with the same velocity v=0.8c, where c is the speed of light (see Figure 3).

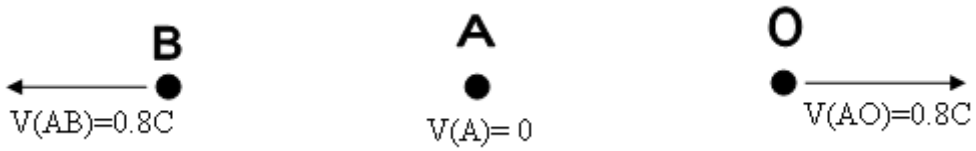

Figure 3. *Schematic classical representation of the motion of points O, A, and B*

In Figure 3, the motion of the points is shown within the framework of classical (Newtonian) mechanics. However, for a more accurate description, let us consider the situation from the perspective of special relativity.

Applying the formula (1) for relativistic velocity addition:

$$V(OB) = \frac{v(OA) + v(AB)}{1 + \frac{v(OA)v(AB)}{c^2}} = \frac{0.8c + 0.8c}{1 + \frac{0.8c \cdot 0.8c}{c^2}} \approx 0.976c$$

For an observer at point O, the relative speed at which point B recedes is approximately $0.976c$.

Since the model is represented as a circle, with its diameter conditionally scaled relative to the limiting speed c, the positions of points A and B along the arc can be determined based on their corresponding relativistic velocities. Thus, the distances along the arcs OA and OB will be proportional to the velocities at which these points recede from O, allowing their positions to be represented on the circle (see Figure 4).

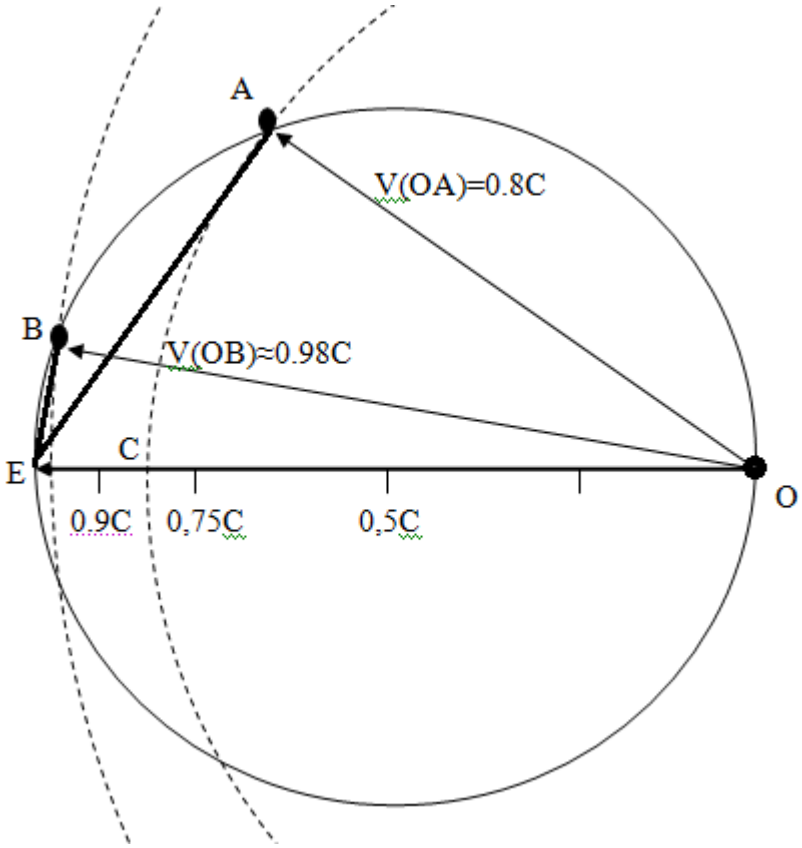

Figure 4. *Geometric visualization of relativistic velocity addition on a circle.*

The figure shows that two right triangles are formed within the circle. According to formula (1), the triangle △OAE represents the position of point A along the arc OE at a speed of $v(OA)=0.8c$, while △OBE reflects the corresponding position of point B along the arc at a speed of $V(OB)\approx 0.976c$. At the same time, based on the initial conditions, it is known that classically, points O, A, and B have a relative speed of 0.8c with respect to each other at this moment.

The relation $v=c=0$ arises not only in the example considered but is also confirmed by other analyses. For example, if one examines points A and B at the critical positions O or E in Figure 1 and sequentially applies the relativistic velocity addition rules, this equality is consistently confirmed.

In classical velocity addition, at the maximal values, one can write:

$V(OB) = V(OA) + V(AB) = c + c$
Taking relativistic velocity addition into account, the formula takes the form:

$$V(OB) = \frac{v(OA) + v(AB)}{1 + \frac{v(OA)v(AB)}{c^2}} = \frac{\mathrm{c} + \mathrm{c}}{1 + \frac{\mathrm{c} \cdot \mathrm{c}}{c^2}} = c$$

Based on the geometric interpretation (Figures 1 and 4), it can also be expressed as:

$$V(OB) = \frac{v(OA) + v(AB)}{1 + \frac{v(OA)v(AB)}{c^2}} = \frac{c + 0}{1 + \frac{c \cdot 0}{c^2}} = c$$

Based on this, one can state that the relative velocity between points A and B can simultaneously be expressed as $V(AB)$=c=0.

It has been known from the very beginning that space is expanding, and the distances between material points increase proportionally to the scale factor. At the same time, relativistic velocity addition introduces an additional correction, which manifests itself in the form of the considered geometric structure.

Thus, v=c=0 is not an artifact of a particular model. It reflects a fundamental property of symmetric geometry, linking extreme states of motion with the characteristics of matter distribution and the structure of the metric.

Moreover, subsequent studies based on gravitational formulas and models of the expanding Universe show that similar patterns recur in various contexts. This further reinforces the physical significance of the result v=c=0.

Such a development naturally raises a question. Does this behavior of matter under extreme conditions suggest the possibility of interpreting the Big Bang as the result of a collision of material points moving at velocities close to the speed of light?

It is precisely this unconventional formulation of the problem that has served as the fundamental basis of the present study. The paradoxical equality of the speeds of three points—confirmed both by relativistic relations and by subsequent analysis—further reinforces its importance.

This development not only reveals a mathematical intrigue but also points to real physical regularities, thereby motivating further investigation into the dynamics of matter under extreme conditions. Although this effect was not explicitly noted in Einstein's classical works, analysis of relativistic formulas confirms its existence.

Why does v=c=0 not violate General Relativity? Water at 0°C turns into ice, yet the laws of thermodynamics are not violated. Something similar may occur here: at v=c, the system transitions into a new state in which the velocity is "zeroed," but energy and momentum are preserved thanks to the underlying geometry.

- Thus, the idea of v=c=0 does not violate General Relativity, and may even complement it if v=c=0 is interpreted not as a literal equality, but as a transition of the system into a new phase state of space-time, where the concepts of velocity, time, and distance are redefined.

This construction clearly demonstrates that relativistic velocity addition is not merely an abstract algebraic rule, but a manifestation of the fundamental geometric structure of space-time. It

naturally arises from the constraints imposed by the Lorentz metric and can be regarded as a reflection of the deep principles of special relativity, embedded in the very nature of motion and interactions of objects at near-light speeds.

5. Analytical dependence of the angle φ on the ratio r/r_s

The angle φ from Figure 1 can be applied in a broader context. It describes not only local gravitational time dilation, but also the generalized degree of spacetime curvature arising in various physical configurations. The previously constructed geometric model allows for the visualization of gravitational effects. It also enables the derivation of analytical relationships between the main physical parameters: radius, gravitational radius, and the curvature angle.

Let us introduce, for example, a normalized quantity $x = \frac{r_s}{r}$. Then, for any gravitational object, one can write: $cos(\varphi) = \sqrt{1 - \frac{r_s}{r}} = \sqrt{1 - \frac{1}{x}},\ \varphi = arccos\left(\sqrt{1 - \frac{1}{x}}\right)$ (2) [14]

This function describes how the angle ϕ — a measure of gravitational curvature — depends on the observer's position relative to a massive body: see Table 1 and Figure 1.

r/r_s	φ (degrees)
1.01	81.1
1.1	71.8
1.5	54.7
2	45.0
3	35.3
5	26.6
10	18.4
100	5.7
∞	0.0

Table 1 – *Dependence of the angle ϕ on the ratio r/r_s – Approximations are rounded to 0.1°*

Table 1, showing the dependence of ϕ on $\frac{r_s}{r}$, illustrates the rapid decrease of space-time curvature with increasing distance from a massive body. As $r \to r_s$, the angle ϕ approaches 90°, reflecting extreme time dilation and maximal gravitational deformation. Conversely, at large r, space becomes nearly flat Graph 1.

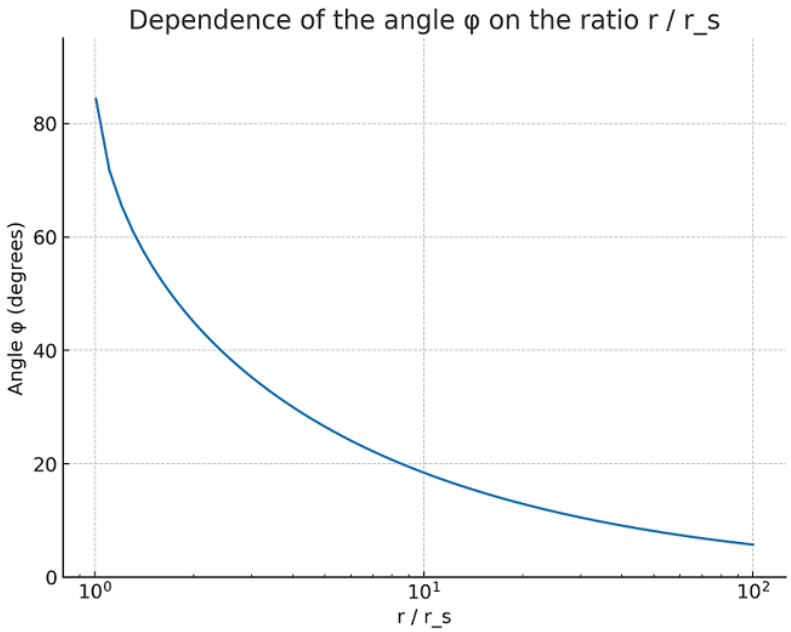

Graph 1 – *Dependence of the angle ϕ on the ratio r/r_s*

6. Geometric Interpretation of Special Relativity Effects

Visualization of relativistic effects, such as length contraction and time dilation, is an important tool for a deeper understanding of the fundamentals of special relativity (SR). The geometric interpretation shown in Figure 5 allows for a clear depiction of the mechanism of relativistic velocity addition.

It also helps to visualize effects such as Lorentz length contraction, as discussed earlier [15].

This approach demonstrates how relativistic changes in space-time characteristics manifest at near-light speeds.

The model's construction provides a tool for interpreting time distortions between two objects moving relative to each other at a constant velocity.

If one object is assumed to remain at rest in its own inertial reference frame, the relative time dilation of the second object can be calculated precisely.

This effect is a key prediction of special relativity and forms the basis of many of its practical applications.

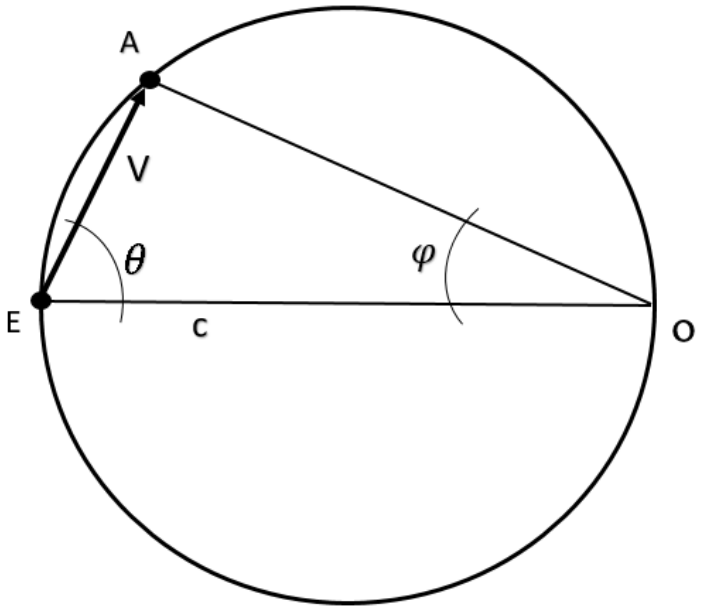

Figure 5 — *a triangle inscribed in a circle*

Suppose that a material point A moves at a constant velocity V relative to the conventionally stationary points E and O. Using trigonometric relationships, one can write:

$$\sin(\varphi) = \frac{V}{C} \text{ (3)}$$

$$\cos(\varphi)^2 + \sin(\varphi)^2 = 1 \text{ (4)}$$

$$\cos(\varphi) = \sqrt{1 - \frac{v^2}{c^2}} \text{ (5)}$$

Thus, the time distortions between points A and E are expressed through the Lorentz factor:

$\Delta t(AE) = t(AE) \cdot \cos(\varphi) = t(AE)\sqrt{1 - \frac{v^2}{c^2}}$ (6) [16].

This geometry can also be interpreted through the Schwarzschild metric for a spherically symmetric massive body:

$ds^2 = -\left(1 - \frac{2MG}{rc^2}\right)c^2dt^2 + \left(1 - \frac{2MG}{rc^2}\right)^{-1}dr^2 + r^2d\theta^2 + r^2sin^2\theta d\phi^2$ (7)

The first factor $\left(1 - \frac{2MG}{rc^2}\right)$ reflects the time dilation in a gravitational field.

In the geometric representation, it can be interpreted as the cosine of the angle of a hypothetical spacetime triangle.

This links gravitational time dilation to the angular characteristics of the figure.
In particular:

$\frac{v^2}{c^2} = \frac{2GM}{rc^2} \Rightarrow \cos(\varphi) = \sqrt{1 - \frac{v^2}{c^2}} \Rightarrow \cos(\varphi) = \sqrt{1 - \frac{2GM}{rc^2}}$ (8) [17]

Depending on the task, it may be more convenient to use sin(φ) instead of cos(φ), or vice versa. This highlights a property of the model: space can be described using either of the trigonometric functions of the angle φ.

Depending on the task, it may be more convenient to use sin(φ) instead of cos(φ), or vice versa.

Such a space can be described using both trigonometric functions of the angle φ. The choice of function is determined by the observer's location—at point O or at point E. In other words, it depends on where and how the observer, in accordance with the symmetry of the metric, establishes their own coordinate system.

Thus, the angle φ serves as a universal variable, reflecting relativistic distortions—time dilation in both general and special relativity, as well as spatial curvature.

In this framework:

• the velocity v is interpreted as a geometric object,

• time dilation is seen as the projection of this velocity,

• gravity is understood as the result of non-coinciding directions of motion in curved space,

• and the inscribed triangle serves as a visual representation of relativistic effects.

Based on equation (8) and, correspondingly, Figure 5, the formula for the second cosmic velocity $v = \sqrt{\frac{2GM}{r}}$ does not merely arise from classical mechanics, but also fits within the relativistic structure of spacetime, including such a geometric interpretation.

The geometric reinterpretation through the angle ϕ allows this relationship to be interpreted as a universal link between Newtonian dynamics, special relativity, and general relativity.

This approach can serve as a conceptual bridge between classical Euclidean geometry and relativistic kinematics.

In the future, it is planned to demonstrate an example - showing how time distortions and velocity changes (Δv) can be expressed through clear visual quantities using this geometry. It is also intended to construct intuitive diagrams to describe complex relativistic scenarios, including GPS navigation effects and orbital motion.

7. Time divergence on a GPS satellite relative to Earth

To verify the scientific validity of the proposed geometric model and its practical application, we consider, as an example, the calculation of the time difference between a satellite clock and an Earth-based clock. This example demonstrates the physical significance of the proposed geometry and its consistency with experimental data from the GPS system. Agreement with actual measurements indicates that all relativistic effects are inherently built into and properly accounted for within this geometric framework.

To verify the applicability of the proposed geometric model in calculating the time difference between a GPS satellite and an observer on the Earth's surface, we perform a step-by-step analysis. Figure 6 illustrates the emergence of this time discrepancy. It is important to note that, although this geometry accounts for all relativistic effects—such as relativistic velocity addition and the Lorentz factor—the model still requires adaptation for each specific case.

In Figure 6, the following notations are used:

O — the center of the Earth.

B — a point on the Earth's surface.
OB — the segment, a leg of the triangle. In this geometry, it corresponds to the Earth's radius and the velocity relative to its center. The Earth's radius can also be associated with the segment-leg EB; in this case, however, the velocity and radius become inversely proportional, which must be taken into account in further calculations.

A — the point on the satellite's orbit. The leg OA represents the distance from the satellite to the center of the Earth and its velocity relative to that center. Similarly, the satellite's orbital radius can be associated with the segment-leg EA; in this case, however, the satellite's velocity and its distance to the Earth's center are also inversely proportional, which should be taken into account in the calculations.

EO — the hypotenuse of both right triangles $\triangle EBO$ and $\triangle EAO$, which we scale to be equal to the speed of light, c. It is important to note that the hypotenuse EO can also be equated to another quantity, which will be discussed in further calculation examples. However, for clarity, we will not overload this paragraph and will focus on the main aspects.

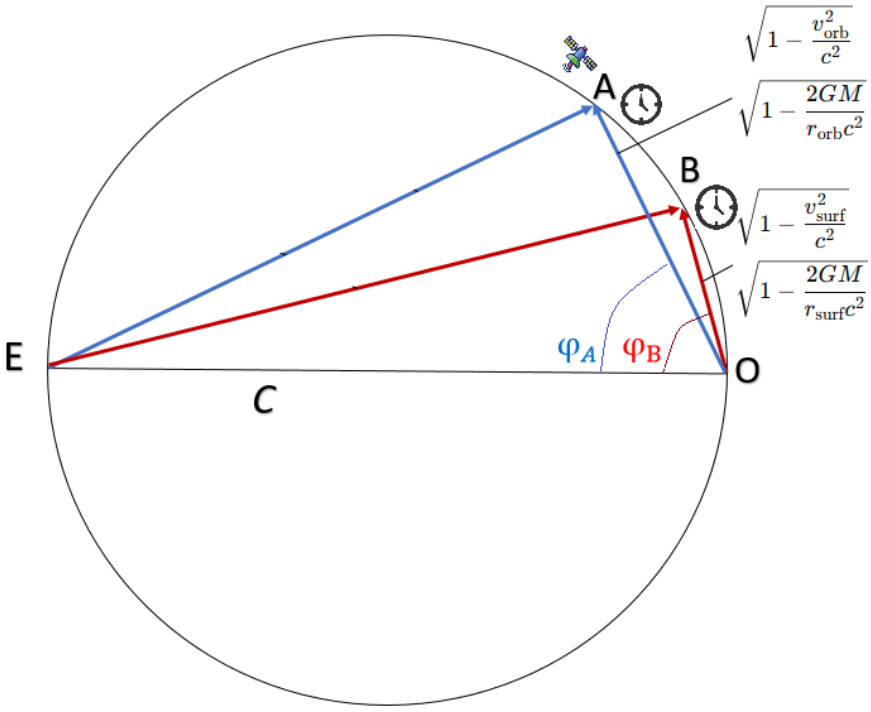

Figure 6 – *Diagram of time divergence on a GPS satellite relative to Earth*

In Special Relativity (SR), moving clocks run slower relative to a given reference frame. We consider this for a GPS satellite in circular orbit and an observer on Earth. Using right triangles inscribed in a circle, the geometric model clearly shows and allows calculation of time dilation as the difference between time-axis projections for different speeds.

In General Relativity, the gravitational field of the Earth and other massive bodies curves spacetime, affecting the passage of time. In the diagram, the legs OB and OE of the triangles illustrate that the Earth's radius is smaller than the satellite's orbital radius. This shows that the gravitational field is stronger on the Earth's surface than at the satellite's orbit, where gravity is

weaker. Therefore, time runs slower on Earth than on the satellite due to the stronger gravitational influence.

By analyzing the legs OB and OE of the triangles, one can also conclude that the kinematic time difference on the satellite, caused by its high speed, is greater than on the Earth's surface. This is because the satellite moves much faster, resulting in stronger kinematic time dilation. Consequently, due to this kinematic effect, clocks on the satellite run slower than those on Earth.

This graphical simplification illustrates how the Earth's gravitational force affects time dilation. On the Earth's surface, time slows down more than in the satellite's orbit. Additionally, the lower speed on the Earth's surface, combined with the higher speed of the satellite in orbit, causes time on the satellite to run slower than on Earth.

Now, let us visualize the dynamics in Figure 6 by considering point A, which represents the satellite's position. The movement of point A along the arc of the circle in both directions symbolizes a change in the satellite's orbit or speed. In this case, the length of the leg of triangle $\triangle EAO$ will change, clearly illustrating variations in the satellite's speed and orbital radius. Accordingly, the angle φ_A, which depends on the position of point A on the circle, will also vary.

Similarly, one can reason about point B on the circle, which represents the leg of triangle $\triangle EBO$. As point B moves along the circle, the speed at the Earth's surface and the Earth's radius change. Accordingly, the angle φ_B, which depends on the position of point B on the circle, also varies.

From this visualization, we can conclude that the kinematic and gravitational time discrepancies between the satellite and the Earth depend on the angles φ_A and φ_B. These angles change according to the positions of points A and B on the circle.

In the first sentence, it should be clearly stated that an increase in the satellite's speed leads to greater time dilation on that satellite. This is because the kinematic effect is directly related to the increase in velocity. Accordingly, the corresponding formula can be written as:
$\Delta t(kin) = \Delta t(AO) - \Delta t(BO) = \Delta t(cos_{kin}(\varphi_A) - cos_{kin}(\varphi_B))$ (9)

In describing the gravitational effect, it should be stated more precisely that time on the satellite runs faster because the satellite is farther from the Earth, where the gravitational influence is weaker. Accordingly, the corresponding formula can be written as:
$\Delta t(grav) = \Delta t(BE) - \Delta t(AE) = \Delta t(cos_{grav}(\varphi_B) - cos_{grav}(\varphi_A))$ (10)
Where Δt is the duration of a day in the Earth-centered frame: Δt = 86,400 s.

Based on formulas (8), this combination can be expressed as follows:

$$\Delta t(kin) = \Delta t\left(\sqrt{1-\frac{v_{surf}^2}{c^2}} - \sqrt{1-\frac{v_{orb}^2}{c^2}}\right) \text{ (11) [18]}$$

$$\Delta t(grav) = \Delta t\left(\sqrt{1-\frac{2GM}{r_{surf}c^2}} - \sqrt{1-\frac{2GM}{r_{orb}c^2}}\right) \text{ (12) [1]}$$

By calculating the time difference using formulas (11) and (12), one can determine the daily discrepancy between the satellite's clock and the clock on Earth, taking into account both the kinematic and relativistic effects. Considering that these discrepancies partially offset each other, the net time difference can be calculated by modifying formula (13):
$T = \Delta t(grav) - \Delta t(kin)$ (13)

$$\sqrt{1-\frac{v_{surf}^2}{c^2}}=\sqrt{1-\frac{465.1^2}{299792.458^2}}\approx 0.9999999999987965\ s$$

$$\sqrt{1-\frac{v_{orb}^2}{c^2}}=\sqrt{1-\frac{3874^2}{299792.458^2}}\approx 0.9999999999165075\ s$$

$$\Delta t(kin)=86400\cdot(0.9999999999987965-0.9999999999165075)=7.11\mu s$$

$$\sqrt{1-\frac{2GM}{r_{surf}c^2}}=\sqrt{1-\frac{2\cdot 6.6743\times 10^{-11}5.972\times 10^{24}}{6371\times 10^3\cdot 299792^2}}\approx 0.9999999993038922s$$

$$\sqrt{1-\frac{2GM}{r_{orb}c^2}}=\sqrt{1-\frac{2\cdot 6.6743\times 10^{-11}5.972\times 10^{24}}{26560\times 10^3\cdot 299792^2}}\approx 0.9999999998330232s$$

$$\Delta t(grav)=86400\cdot(0.9999999993038922-0.9999999998330232s)=45.72\mu s$$

$\Delta t(kin)=7.11\mu s$ — It shows that, due to the kinematic effect, time on the satellite runs slower over the course of a day than on Earth.
$\Delta t(grav)=-45.72\mu s$ — indicates that, due to the gravitational effect, time on the satellite runs faster than on Earth, since the satellite is farther from the center of the Earth, where the gravitational influence is weaker.

Substituting the values into formula (13), we get: $\Delta T=45.72\mu s-\ 7.11\mu s=38.5\ \mu s/s$.

This means that due to the differences in time-dilation effects, the clock on the satellite runs slightly faster than on the surface of the Earth.

The proposed geometric model allows for both quantitative description and clear visualization of relativistic effects, such as kinematic and gravitational time dilation. The calculated results for the time difference between clocks on the GPS satellite and on the Earth's surface confirm that these effects are correctly integrated into the geometric model.

As a result of the combined influence of these two effects, the total time difference between the satellite and the observer on Earth amounts to 38.61 μs. This value matches experimental data obtained during the operation of the GPS system. This demonstrates the high accuracy of the proposed geometric model and its ability to properly account for relativistic effects.

Thus, the model not only theoretically confirms and visualizes known relativistic phenomena. It also serves as a tool for precise calculations of time discrepancies in real physical systems, such as satellite navigation systems.

The accuracy of the model demonstrates that it can also be adapted for other relativistic calculations, while taking into account the specific features of each task for correct application.

8. Geometric explanation of the relationship between the angle φ and gravitational time dilation

As has been shown, the angle φ allows one to express the time discrepancy between a satellite

and an observer on the Earth's surface. However, to gain a deeper understanding of the physical nature of this relationship, it is necessary to examine the geometric meaning of the angle φ and its connection with general relativity.

In the previously proposed model, the angle φ is defined by the expression: $\cos(\varphi) = \sqrt{1 - \frac{r_s}{r}}$ (14) which formally coincides with the gravitational time dilation factor in the Schwarzschild metric: : $d_\tau = dt \cdot \sqrt{1 - \frac{r_s}{r}}$ (15), [17], Where $d\tau$ is the proper time, dt is the coordinate time, and r_s is the gravitational radius.

This coincidence is not accidental. In the geometric interpretation, the angle ϕ corresponds to the tilt of an observer's time in curved spacetime relative to time in flat (global) space. As one approaches the gravitational object $r \to r_s$, the angle ϕ approaches 90° (see Graph 2), which corresponds to a complete "freezing" of time relative to a distant observer.

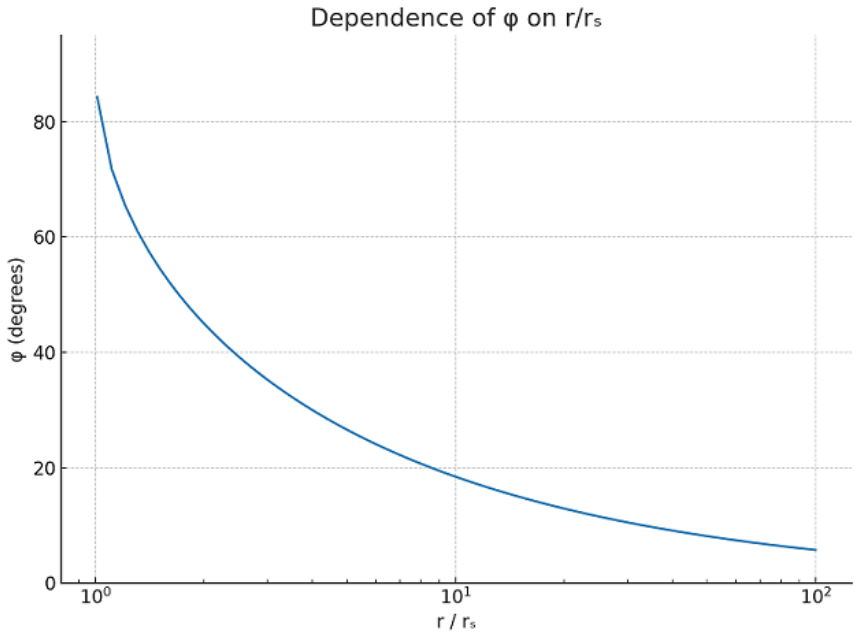

Graph 2 — *Dependence of the angle φ on the ratio* $\frac{r_s}{r}$

This quantity combines local curvature characteristics (through r/r_s) with the global consequences of spacetime curvature.

The geometric model based on the angle φ clearly illustrates how time dilation increases as one approaches massive gravitational objects. The expression $\cos(\varphi) = \sqrt{1 - \frac{2GM}{rc^2}}$ (8) appears in the Schwarzschild metric as the coefficient of dt — where $r_s = \frac{2GM}{c^2}$ the Schwarzschild radius. It becomes evident that as $r \to r_s$, $\cos(\varphi) \to 0$ and $\varphi \to 90^\circ$ [18] (see graph 2). This limiting value of the angle reflects a physical boundary: complete gravitational time dilation, where clocks near the event horizon appear to "stop" from the perspective of a distant observer.

The angle φ can be interpreted as the angle between the time axis of a distant observer and the proper-time vector of a local observer. This geometric deviation reflects how gravity warps space-time: the closer an object is to the gravitational source, the more its worldline deviates

from the coordinate time axis.

This picture aligns well with the predictions of General Relativity and provides a clear explanation of why a GPS satellite, orbiting at a higher altitude, experiences time passing faster than on the Earth's surface. Its angle φ is smaller, meaning the deviation from 'true time' is weaker.

Thus, the angle φ is not merely a formal parameter. It is a geometrically meaningful quantity connected with the fundamental properties of space-time and with time dilation in a gravitational field. The angle φ can be regarded as a key parameter describing not only spatial geometry but also temporal distortions in gravitational systems.

Continuing the interpretation proposed in the previous section, it becomes a natural bridge between geometric constructions and the physical effects of time curvature.

This behavior of φ can be compared to the Lorentz factor in special relativity: as $v \to c$, time also “stops”—not due to gravity, but due to motion. This suggests that the angle φ can serve as a universal geometric indicator of extreme states, encompassing both relativistic and gravitational limiting effects.

Therefore, the geometric interpretation of φ provides not only a visual but also an analytical tool for describing strong gravitational fields, event horizons, and potentially even new extreme regimes that go beyond the classical formulas.

9. Analytical dependence of the orbital eccentricity on the angle φ

1. Introduction

The orbital characteristics of the planets in the Solar System can be described using various physical parameters, including orbital eccentricity and orbital velocities. Within the framework of general relativity, the curvature of space-time affects orbital motion, and this effect can be represented using a geometric model based on the angle φ. This angle φ, reflecting the degree of space-time curvature, can be related to a planet’s orbital eccentricity and its orbital velocity.

In this relativistic model, the mathematical dependence of the angle φ on the orbital eccentricity and velocities of planets is considered, as well as the influence of gravitational curvature on orbital dynamics.

In the course of this study, a remarkable phenomenon can be observed: variations of the angle φ and their impact on the orbital velocities of planets obey the principle of mirror symmetry. This observation paves the way toward a deeper understanding of the fundamental interrelation between matter, energy, and gravity in such a space. For clarity, we shall analyze the eccentricities of planetary orbits, demonstrating the specifics of such calculations and their connection with the proposed geometric model. This approach makes it possible to highlight a key final result directly linked to the peculiarities of the given geometry.

2. Geometric Model and Its Relation to Eccentricity

The exploration of the relationship between orbital eccentricity and the angle φ begins with the formula for the eccentricity of an elliptical orbit, which is defined through the orbit’s semi-major and semi-minor axes: $\varepsilon = \sqrt{1 - \frac{b^2}{a^2}}$ (16) — where a is the semi-major axis of the orbit, and b is the semi-minor axis. However, in this case, for orbits that are not perfectly circular, the angle ϕ is used as a parameter to

describe the degree of space-time curvature, and we can express the eccentricity through the geometric angle ϕ as: $\cos(\varphi) = \sqrt{1 - \frac{r_s}{r}} = \sqrt{1 - \frac{1}{\chi}}$, $\varphi = arccos\left(\sqrt{1 - \frac{1}{\chi}}\right)$ (17) — where r_s — is the gravitational radius, r — is the distance from the center of mass, and χ — is the normalized quantity defined as $\chi = r_s/r$.

3. Orbital velocities and their dependence on the angle φ

To calculate the orbital velocities of the planets, two approaches were used.

First, the orbital velocity was calculated using the classical gravitational formula, which provides the basic orbital speed [18]: $v_0 = \sqrt{\frac{GM}{r}}$ (18) — where G is the gravitational constant, M — the mass of the Sun, and r — the distance from the planet to the Sun.

The curvature of spacetime was taken into account by calculating the "corrected orbital velocity" through the angle φ: $v_{\text{corrected}} = v_0 \cdot \cos(\varphi)$ (19) where $\cos(\varphi)$ reflects the degree of curvature associated with the eccentricity of the orbit.
$G = 6.674 \times 10^{-11} m^3 kg^{-1} s^{-2}$
$M = 1.989 \times 10^{30} kg$

$r = 5.791 \times 10^{10} m$

$$v_0 = \sqrt{\frac{6.674 \times 10^{-11} \cdot 1.989 \times 10^{30}}{5.791 \times 10^{10}}} \approx 47884.94 m/s$$

Within the framework of this analysis, the angle φ is used to adjust the orbital velocity, introducing a correction analogous to the effects of general relativity. This approach makes it possible to relate the parameters of an elliptical orbit (including its eccentricity) to the magnitude of relativistic distortion, mediated through the angle φ.

A direct calculation using $\cos(\varphi)$ for certain planets (for example, Mercury) produced inadmissible values lying outside the physically acceptable range. To resolve this issue and obtain consistent velocities, we employed $\sin(\varphi)$, which physically corresponds to the factor representing the influence of spacetime curvature on the orbital velocity. The proposed approach will receive its physical and geometric justification in further studies.

$$\sin(\varphi) = \sqrt{1 - cos^2(\varphi)} = \sqrt{\frac{1}{\chi}} = \sqrt{\frac{r_s}{r}} \approx 0.9789$$

r_s — gravitational radius of the Sun for the planet

r — distance from the planet to the Sun

$v_{\text{corrected}} = v_0 \cdot \sin(\varphi) = 47884.94 \cdot 0.9786 \approx 9845.14 m/s$
$\triangle v = v_0 - v_{\text{corrected}} = 47884.94 - 9845.14 \approx 38039.8 m/s$

Verification of the connection with eccentricity:

The known eccentricity of Mercury is: ϵ=0,2056

$$\sin(\varphi) \approx \sqrt{1-\epsilon^2} \approx 0.9786 \Rightarrow \epsilon = 0{,}2056$$

4. Results and Analysis

For each planet in the Solar System, both the basic and corrected orbital velocities were calculated (see Table 2). The results obtained using this geometric approach showed that planets with low eccentricity (for example, Earth and Venus) exhibit minimal changes in orbital velocity. In contrast, for planets with high eccentricity (for example, Mercury and Pluto), the difference between the basic and corrected velocities increases significantly.

The table below presents the orbital velocity results for the planets, calculated both using the gravitational field and taking into account the gravitational curvature described through the angle φ.

Planet	Base orbital velocity (m/s)	Corrected speed (m/s)	Speed difference (m/s)	Eccentricity (ε)	sin(ϕ)
Mercury	47884.94	9845.14	38039.8	0.2056	0.9786
Venus	35033.64	238.23	34795.41	0.0068	0.99998
Earth	29788.9	497.47	29291.42	0.0167	0.99986
Mars	24130.26	2253.77	21876.49	0.0934	0.9956
Jupiter	13059.53	638.61	12420.92	0.0489	0.9988
Saturn	9646.03	545.0	9101.03	0.0565	0.9984
Uranus	6799.95	314.84	6485.11	0.0463	0.9989
Neptune	5432.44	46.72	5385.72	0.0086	0.99996
Pluto	4740.84	1179.52	3561.32	0.2488	0.9686

Table 2 — *Planetary velocities and the relationship with eccentricity (ε)*

Alignment of eccentricity: sin(φ) = 0 and sin(φ) = 1

An important aspect of the model is how the orbital eccentricity aligns in the extreme cases, when the curvature of space-time is minimal or maximal.

This occurs in the following situations:

1. When sin(φ) = 0 — circular orbit:

In this case, the angle φ equals zero, which corresponds to an orbit with eccentricity ε = 0, i.e., a perfect circular orbit. Here, space-time is not curved, and the planet's orbital velocity remains constant along the entire orbit. The difference between the basic orbital velocity and the corrected velocity will be zero, since sin(φ) = 0. There is no need to adjust the velocity due to gravitational curvature. In this scenario, the planet's orbital speed is at its maximum and is not limited by other factors, such as space-time curvature.

2. When sin(φ) = 1 — maximum curvature:

When the angle φ equals 90° (corresponding to the maximum curvature of space-time), the difference between the basic and corrected orbital velocities reaches its maximum. This is typical for planets with eccentricities close to one, such as Mercury or Pluto, where the orbital speed varies significantly depending on the planet's position in its orbit. In this case, when φ = 90°, the gravitational curvature of space-time strongly affects the planet's velocity, and the difference between the basic and corrected speed is at its maximum. This confirms that for sin(φ) = 1, a planet's orbital velocity can approach the maximum theoretical speed, such as the speed of light, as shown in models with extreme curvature.

Hypothesis on Space Symmetry

From the above, an interesting suspicion or hypothesis arises: the two cases, when sin(φ) = 0 and sin(φ) = 1, may describe the same state or moment in space, but with different interpretations. In both cases, space-time experiences extreme conditions: either a complete absence of curvature or a maximally pronounced curvature. However, the question arises as to why we observe such differences, despite the possible identity of the underlying state.

This hypothesis can, for example, be explained through the symmetry of space, which ensures the unity and interconnection of these extreme cases. Thus, it can be proposed that the transition from sin(φ) = 0 to sin(φ) = 1 represents a single sequence of events connecting the two limiting states. In this view, the orbital eccentricity of a planet and gravitational curvature can be interpreted as two aspects of the same physical reality, which requires a deeper logical explanation.

This sequence can be understood through the existence of spatial symmetry, which unites various gravitational and kinetic effects into a single model. This unification opens new possibilities for further research.

In the previous analysis, we reached an important conclusion: for the value sin(φ) = 0, the orbital velocity of the planet was set equal to the speed of light, c=299,792,458 m/s (see Table 3). This result has a profound physical interpretation, which deserves a more detailed discussion.

Planet	Base Orbital Speed (m/s)	Corrected Speed for sin(φ)=0 (m/s)	Corrected Speed for sin(φ)=0.707 (m/s)	Corrected Speed for sin(φ)=1 (m/s)
Mercury	47884.94	299792458	33854.65258	0
Venus	35033.64	299792458	24768.78348	0
Earth	29788.9	299792458	21060.7523	0
Mars	24130.26	299792458	17060.09382	0
Jupiter	13059.53	299792458	9233.08771	0
Saturn	9646.03	299792458	6819.7432100000005	0
Uranus	6799.95	299792458	4807.564649999999	0
Neptune	5432.44	299792458	3840.7350799999995	0
Pluto	4740.84	299792458	3351.7738799999997	0

Table 3 — *Orbital velocities for sin(ϕ) = 0, sin(ϕ) = 0.707 and sin(ϕ) = 1*

When we talk about the situation where sin(ϕ)=0, this means there is no curvature of space-time. Within the framework of general relativity and the curved space-time model, this leads to a state in which the planet's orbital velocity reaches its maximum possible value. Under such conditions, this maximum speed can be associated with the fundamental limit imposed by the speed of light.

This explanation can also be interpreted in the context of hypothetical cosmological scenarios. In such scenarios, the absence of space-time curvature may lead to a maximum velocity equal to the speed of light. This case illustrates an extreme state in which the speed of objects reaches the ultimate limit set by the speed of light.

We can view this result as a manifestation of the symmetry of space. When curvature is absent, objects achieve the ultimate speed—the speed of light—thus creating a theoretical foundation for further research in the fields of gravity.

Now, let us consider the case when sin(φ) = 1. This sine value corresponds to the maximum curvature of space-time, when the angle φ = 90°. In this situation, space-time becomes maximally curved, and the planet's orbital velocity approaches zero, indicating extreme conditions such as the event horizons of black holes.

Let us compare the two extreme cases — sin(φ) = 0 and sin(φ) = 1. We can observe that in the absence of curvature, when sin(φ) = 0, the planet's orbital velocity is maximal and equals the speed of light, c.

However, under maximum curvature, when sin(φ) = 1, the orbital velocity approaches zero, reflecting a process in which the gravitational field becomes so strong that the motion of the object effectively stops from the perspective of a distant observer.

These two — sin(φ) = 0 and sin(φ) = 1 extreme cases represent opposite limiting states and provide a unique insight into how the motion of objects changes depending on the gravitational

field and the curvature of space-time.

This contrast between the two states—where a planet's velocity is either maximal (sin(φ) = 0) or minimal (sin(φ) = 1)—opens up new opportunities for further research in the fields of relativity theory and quantum gravity.

In the calculations, we will replace sin with cos and observe the results (see Table 4):

Planet	**Base Orbital Speed (m/s)**	**Corrected Speed for cos(φ)=0 (m/s)**	**Corrected Speed for cos(φ)=0.707 (m/s)**	**Corrected Speed for cos(φ)=1 (m/s)**
Mercury	47700.414520783204	0	33724.19306619372	299792458
Venus	35106.55452268914	0	24820.334047541222	299792458
Earth	29788.8993205065	0	21060.751819598096	299792458
Mars	24161.987908468855	0	17082.525451287478	299792458
Jupiter	13063.29651768997	0	9235.750638006808	299792458
Saturn	9624.356512541948	0	6804.420054367157	299792458
Uranus	6800.126147280675	0	4807.689186127437	299792458
Neptune	5432.349991416317	0	3840.6714439313355	299792458

Table 4 — *Orbital velocities for different values of cos (ϕ) = 0, cos(ϕ) = 0.707 and cos(ϕ) = 1*

This table illustrates the orbital velocities of planets for different values of the cosine of the angle φ, which represents the degree of space-time curvature:

1. Cos(φ) = 0: In this situation, the orbital velocity is zero, corresponding to the maximum curvature of space-time (for example, at the event horizon of a black hole), where motion becomes impossible.

2. Cos(φ) = 0.707: The orbital velocity is calculated as $v_{ext} = v_{max} \times 0.707$, corresponding to a state where space-time is curved to a significant extent, but motion of the object is still possible.

3. Cos(φ) = 1: Here, the orbital velocity equals the maximum orbital speed for a given orbit, reflecting the situation where space-time is not curved, and the object moves along its orbit according to classical Newtonian mechanics.

Tables 3 and 4 help illustrate how variations in the angle Φ (and, consequently, the curvature of space-time) affect the orbital velocities of planets.

Within the framework of examining the dependence of orbital velocities on the angle ϕ, we observe an interesting symmetry between the values of sin(ϕ) and cos(ϕ), which manifests as a

mirror symmetry of the processes. This becomes apparent when we analyze the corresponding values for sin(ϕ) = 0, sin(ϕ) = 0.707, and sin(ϕ) = 1, as well as for cos(ϕ) = 0, cos(ϕ) = 0.707, and cos(ϕ) = 1 (Tables 3 and 4), and notice that they appear in reverse order.

The key point is that for the value sin(ϕ) = cos(ϕ) = 0.707, all orbital velocity parameters coincide. This can be interpreted as an indication of mirror symmetry in such a space-time geometry. The "mirror" position is precisely at the point where sin(ϕ) = cos(ϕ) = 0.707, which may indicate a special balance in the space-time curvature that leads to the coincidence of these values.

This mirror symmetry in the metric or space-time geometry may imply that a fundamental symmetry exists within such a system, explaining the interrelation between different states of matter and energy. In this context, the difference between the processes occurring at sin(ϕ) = 0 and sin(ϕ) = 1, as well as between the states cos(ϕ) = 0 and cos(ϕ) = 1, becomes clearer.

Moreover, the results obtained for the proposed geometry allow us to explain the unusual behavior of orbital velocities as they approach the extreme values v=0 and v=c. In the standard interpretation, the speed of light v=c is unattainable for an object with nonzero mass. However, within the framework of a symmetric metric, this limitation loses its traditional meaning, leading to the formulation of the so-called "critical state" v=c=0.

In such a symmetric metric, the speed of light no longer represents an insurmountable limit, but rather a transitional state in which all matter and energy transform into a new state. This suggests that while in the conventional metric it is impossible for matter to reach the speed of light, in a metric with symmetry, space-time adapts. This makes the transition possible, where the speed of light c effectively becomes the rest state for matter.

In the space-time geometries we are studying, mirror symmetry plays a key role. When we analyze the results for sin(ϕ) and cos(ϕ), this mirror symmetry becomes apparent, allowing us to draw an important conclusion: the process by which a planet's orbital speed approaches the speed of light or tends toward zero is not accidental, but rather a result of a fundamental symmetry embedded in the structure of such space-time.

Thus, in this hypothetical interpretation of space, the problem of the impossibility of exceeding the speed of light in classical relativity disappears. We obtain a more complete understanding of the behavior of matter under extreme conditions, as well as the interconnection of various physical processes within a symmetric geometry.

In a sense, within such a geometry, an incredible yet important question arises: could the so-called Big Bang be the result of a state where v=0=c? This special state might characterize the simultaneous existence of matter and antimatter. The interaction between these two states could serve as a link between the limits of the speed of light and its absence.

Thus, in this geometry, the Big Bang may not be merely a beginning. Rather, it could represent a transitional state in which the boundary between matter and antimatter disappears, and space-time undergoes fundamental transformations.

10. Investigation of the Sun's radius using the angle Φ and the advantage of a mirror-symmetric calculation

Let us move on to a further analysis from the perspective of a purely gravitational approach. In this section, we examine the dependence of the angle Φ on the radius *R* [1, 6], using the formula for the cosine of the angle:

$$\cos(\varphi) = \sqrt{1 - \frac{2GM}{Rc^2}} \quad (8)$$

Here:
- G — Gravitational constant,
- M — mass of the Sun,
- R — radius of the Sun,
- c — speed of light.

We will vary the angle Φ from 0° to 90° in steps of 10° to understand how the radius R of the Sun changes for different values of the angle.

Example of a numerical calculation: For the Sun's radius R=696,340 km, we calculate the angle Φ using the formula mentioned above:

Substitute the given values:

$$\cos(\varphi) = \sqrt{1 - \frac{2 \times 6.67430 \times 10^{-11} \times 1.989 \times 10^{30}}{696.34 \times 10^{6} \times (3 \times 10^{8})^{2}}} \approx 0.99999788$$

The result for the angle Φ is 0.118° for the actual radius of the Sun, 696.34×10^{6}.

We will investigate the dependence of the radius *R* on the angle Φ from 0° to 90° with a step of 10°. Following the logic, the studied radius R can be determined using formula (20), and the results are presented in Table 5:

$$R = \frac{2GM}{c^2} \cdot \cos^2(\Phi) \quad (20)$$

Using formula (20), we obtain the radius values shown in Table 5, which correspond to Graph 3.

Angle Φ (degrees)	Radius R (km)
0	2.95
10	3.04
20	3.34
30	3.93
40	5.03
50	7.14
60	11.8
70	25.22
80	97.83
90	7.87e+32

Table 5 — *Radius R for angles from 0° to 90° with a step of 10°*

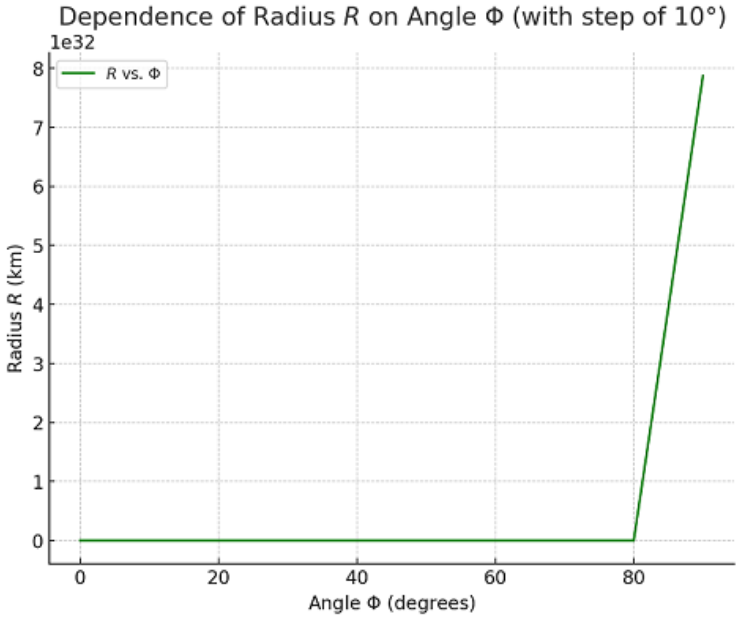

Graph 3 — *Dependence of radius R on angle Φ*

We have plotted Graph 3, showing the dependence of radius R on angle Φ from 0° to 90° with a step of 10°. The graph demonstrates how the radius decreases as the angle Φ decreases, approaching the Schwarzschild radius when Φ=0°. However, starting from Φ=80°, the radius sharply increases. This behavior can be explained by the fact that at large values of Φ, the curvature of space-time becomes more pronounced, causing the radius to tend toward very large values.

Conclusions:

As the angle Φ decreases, the radius R decreases and approaches the Schwarzschild radius, which is approximately 2.95 km for the Sun.

As the angle Φ increases, the radius R significantly increases, corresponding to weak space-time curvature at large distances. At Φ=80°, the radius sharply increases. This occurs because, at these angle values, the space-time curvature becomes minimal, and the radius begins to approach "infinity."

To study the symmetric metric, we replace cosine with sine in the formula, adapting our model to a symmetric metric.

We replace cosine with sine in the original formula (20) and obtain the modified formula (21):

$$\sin(\Phi) = \sqrt{1 - \frac{2GM}{Rc^2}} \quad (21)$$

This will give us the dependence of the radius R on the angle Φ for the symmetric metric.
Let's calculate the radius R [1,6] for angles from 0° to 90° in 10° increments using the modified formula:

$$R = \frac{2GM}{c^2} \cdot \sin^2(\Phi) \quad (22)$$

Formulas (20) and (22) represent the expression of the radius through trigonometric functions for the chosen metric.

We expect the changes to be symmetric, with the radius varying similarly but following a different dependence (sine instead of cosine).

We recalculate and plot the graph for this symmetric metric.

For the symmetric metric, formula (22) gives the values shown in Table 6, which are illustrated in Graph 4.

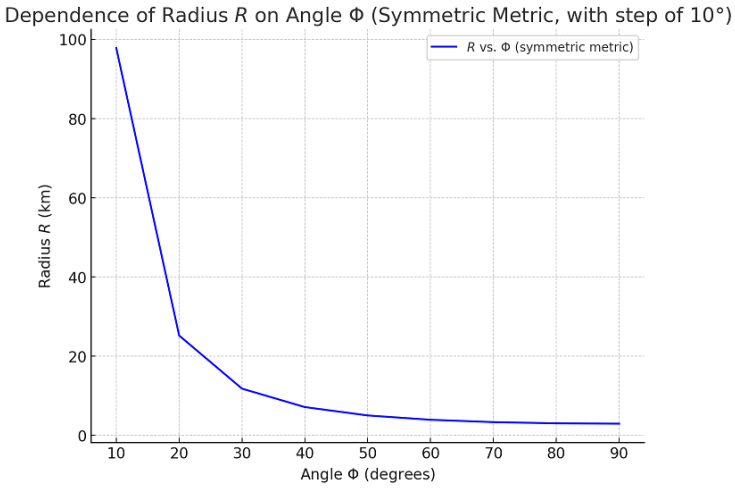

Graph 4 — *Dependence of radius R on angle Φ for the symmetric metric.*

At $\Phi = 0°$, the radius R becomes infinite, which is due to the fact that sin=0°, and we are dividing by zero.

As the angle increases, the radius begins to decrease, but it changes symmetrically compared to the original metric (with cos).

This confirms the idea of a symmetric change in the metric: by replacing cosine with sine, the behavior of the radius also changes symmetrically.

Angle Φ (degrees)	**Radius R (km)**
0	$\cos(\Phi)=\infty \leftrightarrow \sin(\Phi)=7.87 \times 10^{32}$
10	97.83
20	25.22
30	11.8
40	7.14
50	5.03
60	3.93
70	3.34
80	3.04
90	2.95

Table 6 — *Radius R for angles from 0° to 90° with a step of 10° for the mirror-symmetric metric*

Interestingly, when transitioning between mirror-symmetric calculations, for example, from cosine to sine, we can avoid the difficulties associated with division by zero. This is similar to the problem encountered with the speed of light, where it is necessary to interpret that no object with mass can reach the speed of light. In relativistic physics, this is due to the fact that for objects with nonzero mass, an infinite amount of energy is required to reach the speed of light [16, 19].

Thus, there are physical problems where division by zero leads to mathematical difficulties. Similar limitations and concepts are physically inexplicable for objects with mass attempting to reach the speed of light.

So, these two phenomena—division by zero in mathematical calculations and the impossibility of reaching the speed of light for objects with mass—represent important constraints that we must take into account in our models. These limitations indicate the existence of inherent boundaries—whether in mathematical computations or in the physical realities described by relativistic theory. At the same time, symmetric calculations help us avoid extreme values, such as infinities, providing a clearer and more comprehensible picture of physical reality.

However, considering the symmetric approach, we see that when using the cosine for the angle $\Phi = 90°$, the radius tends toward a value on the order of 7.87×10^{32}, which corresponds to an

unusual, yet well-defined result. Thus, it can be argued that in our problem, using mirror-symmetric calculations, infinity can be replaced by an appropriately finite value: $\cos(\Phi) = \infty \leftrightarrow \sin(\Phi) = 7.87 \times 10^{32}$. This notation emphasizes the mirror-like relationship between the cosine and sine metrics: where one formally tends to ∞, the other attains a finite, though very large, value.

This suggests that infinity, in the context of this metric, is not an abstract concept. Rather, it symbolizes an extremely large value of the radius, which is reflected in the numerical results when using symmetry.

The symmetry between the cosine and sine metrics illustrates that physical constraints (for example, the Schwarzschild radius) remain constant. The extreme values are merely mathematical features of the chosen trigonometric function.

The importance of symmetry and mirror calculations

Interestingly, when transitioning between mirror-symmetric calculations, for example, from cosine to sine, we can avoid difficulties with division by zero. When a zero appears in the numerator, as happens with sine at $\Phi = 0°$, in the mirror-symmetric calculation using cosine, we obtain a definite value. This allows us to bypass this mathematical issue.

This provides a clear advantage when using symmetry in calculations. In cases where calculations with one trigonometric function (for example, sine) encounter division by zero, the mirror-symmetric calculation using cosine—or vice versa—yields more stable results, avoiding mathematical difficulties.

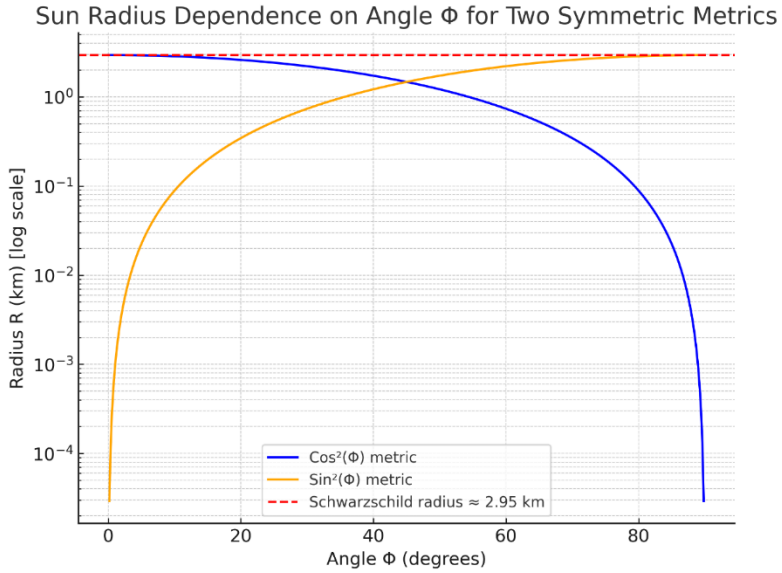

Graph 5 — *for the Sun with two metrics — using cos(Φ) and sin(Φ).*

Red dashed line—Schwarzschild radius (~2.95 km), blue line—cosine metric (rises sharply as $\Phi \to 90°$), orange line—sine metric (tends to infinity as $\Phi \to 0°$, then quickly decreases toward the Schwarzschild radius). The mirror-like reflection of the dependencies is clearly visible, demonstrating the advantage of the symmetric approach.

Conclusions:

- At Φ = 0° when using the sine metric, we encounter a computational difficulty due to division by zero, which leads to infinity.
- In contrast, when calculating with the cosine metric for Φ = 90°, the radius approaches an extremely large value of 7.87×10^{32}, which can be interpreted as representing infinity in this symmetric metric. Most likely, 7.87×10^{32} corresponds to the maximum radius of the Sun's metric.
- The transition between mirror-symmetric calculations allows us to bypass difficulties arising from division by zero, making the mathematical models more flexible and stable.
- We encountered a similar necessity when calculating the orbital eccentricities of planets. A simple mirror-symmetric approach allowed us to equate the speed of light, v=c=0, with zero velocity. It should be emphasized that in this analysis, as clearly shown in Figure 4, significant importance is given to cos(45°)=sin(45°)≈0.707 — $v = c \cdot \sin(45^{\circ}) = \frac{c}{\sqrt{2}} \approx 0{,}707c$.
- Thus, the symmetric approach helps resolve computational difficulties—providing more accurate and logical results in the context of relativistic effects and beyond. The physical justification of this method will become clearer in subsequent studies.

11. Resolving Infinity and the Speed Limit through Mirror Symmetry

In classical special relativity, the energy of a particle with mass m, moving at a velocity v, is given by the formula:

$E = \gamma mc^2$ (23), where $\gamma = \frac{1}{\sqrt{1-\frac{v^2}{c^2}}}$(24)

As $v \to c$, the denominator in the Lorentz formula approaches zero, and the energy formally tends to infinity [20, 21, 22]. This limitation reflects the physical impossibility for material objects to reach or exceed the speed of light in a vacuum. However, this expression may indicate a mathematical singularity rather than a physical event.

Here, we encounter the problem of singularity, where the mathematical model predicts an infinite energy value, which is physically unrealizable. This highlights the need to revise or extend the existing model.

Rethinking the Speed of Light Limit through Mirror Symmetry

Let us consider an extended space-time geometry taking mirror symmetry into account.

The introduction of the parameter ϕ allows us to use trigonometric functions to describe the velocity as a function of the angle. This simplifies the analysis of limiting cases:

$$v = csin(\varphi)$$

Then the Lorentz factor can be rewritten as:

$$\gamma = \frac{1}{\sqrt{1-\frac{v^2}{c^2}}} = \frac{1}{\sqrt{1-sin^2(\varphi)}} = \frac{1}{\cos(\varphi)} \quad (25)$$

Using the trigonometric identity $\cos(\varphi)^2 + \sin(\varphi)^2 = 1$, we simplify the expression for the Lorentz factor, which makes it easier to analyze its behavior for different values of φ.

The classical limit $v \to c$ corresponds to $\varphi \to 90^{\circ}$, where $\cos(\varphi) \to 0$ and the energy tends to infinity:

$$E = \frac{mc^2}{\cos(\varphi)} \to \infty \ (26)$$

However, the introduction of mirror space implies that in this symmetric world the angle transforms as $\varphi' = 90^{\circ} - \varphi$, so that for $\varphi = 90^{\circ}$ in the mirror space $\varphi' = 0^{\circ}$. In this case, the particle's energy in the mirror world is given by:

$$E' = \frac{mc^2}{\cos(\varphi')} = \frac{mc^2}{\cos 0^{\circ}} = mc^2 \ (27)$$

That is, it takes a finite and physically interpretable value [23].
At $\varphi = 90^{\circ}$, the particle's velocity reaches the speed of light, and its energy tends to infinity, corresponding to the classical singularity. In the mirror space, the angle φ complements φ to 90°, which allows us to analyze the system's behavior in the symmetric world.

In mirror symmetry, the angle φ in one space is related to the angle φ' in the symmetric space, where $\varphi' = 90^{\circ} - \varphi$. This means that when the velocity in one space approaches the speed of light, in the mirror space the object transitions to a state of rest.

In the mirror space, at $\varphi' = 0^{\circ}$, the particle's energy takes the finite value mc^2, corresponding to the particle's rest energy. This resolves the singularity problem and offers a new interpretation of the speed of light limit.

Thus, reaching the speed of light in our geometric space is not an unattainable limit. Instead, it represents a phase transition.

During this transition, the object moves to a state of rest in the mirror space. This provides a new physical interpretation of the speed of light limit. Through mirror symmetry, the speed of light limit represents a transition between two "states" of space.

Phase Transition and Mirror Symmetry of Velocities

Through mirror symmetry, we observe that reaching the speed of light in our space ($v \to c$) corresponds to a transition to a state of rest ($v' = 0$) in the mirror space.

Interestingly, mirror symmetry also allows us to consider the reverse sequence:

$$E_{peace,our\ world} = E_{speed\ of\ light,mirror\ world} \Leftrightarrow E_{speed\ of\ light,our\ world} = E_{peace,mirror\ world}$$

In other words, the rest energy and the energy at the speed of light are the same when viewed through the symmetry of spaces. This principle also implies that both zero velocity and the speed of light can coexist, but our metric perceives only one of these states directly.

Physical Meaning

In this geometry, the speed of light limit ceases to be an unattainable boundary. It becomes a phase transition between interconnected worlds, where the energy remains finite and the classical singularity disappears.

This Opens New Possibilities:

- Theoretical investigations — modeling phase transitions between worlds.
- Experimental tests — for example, through colliders, mirror symmetries, and new metrics, one can study the manifestations of energy and velocity in both metrics.
- Visualization of the simultaneous existence of zero velocity and the speed of light—new approaches to understanding the limits of special relativity.

Although we cannot literally observe the "mirror world," its symmetries can be modeled through new metrics and mathematical transformations. High-energy experiments, colliders, and analogous systems can help test whether the predictions of such a geometric model are consistent with the observed energy and velocity of particles in our metric [24]. Thus, mirror symmetry becomes a tool for theoretical verification and modeling, rather than direct observation of another world.

Illustrative Examples

Our world: the particle is at rest (v=0), with energy $E= mc^2$.

Mirror world: the same particle moves at the speed of light (v=c), with the same energy = mc^2.

Conclusion: the energy remains finite, and motion is a relative concept, depending on the observer's point of view.

Logical "Test"

- The rest energy in our world = the energy at the speed of light in the mirror world.
- The rest energy in the mirror world = the energy at the speed of light in our world.

Therefore, the energy is always finite; velocities 0 and c are two states of the same object, observed through different metrics.

Physical Meaning

Thus, reaching the speed of light in our geometric space corresponds to a transition to a state of rest in the mirror space. This eliminates the classical energy singularity and provides a new physical interpretation of the speed of light limit—not as an unattainable boundary, but as a phase transition between two interconnected worlds. This opens new possibilities for theoretical studies and experimental verification.

Reaching the speed of light under ordinary conditions in our space is impossible. However, such a geometry shows that it becomes possible in the limit of extreme situations, for example, near a light singularity, such as the Schwarzschild radius. Therefore, for conclusive verification and experiments, the focus should be on extreme conditions. It is precisely there that mirror symmetry and the phase transition of energy and velocity manifest. This can be studied not only mathematically but also through artificially created physical scenarios.

In this geometry, the concept of the speed of light limit ceases to be a forbidden boundary. It is a phase transition between two interconnected worlds, where physical quantities remain finite and meaningful.

- The classical energy singularity disappears.
- The speed of light limit acquires a new interpretation.
- Experimental verification is possible through mirror symmetries and new metrics.

- Zero velocity and the speed of light can simultaneously exist in the same system if the geometry of space and mirror symmetry are taken into account.

12. Mathematical development of geometry and experimental verification

For the completeness of the model, it is necessary to develop the mathematical framework, including:

- Modification of the Hamiltonian formalism, taking into account the dependence of mass and other parameters on the angle ϕ [25];
- Investigation of the smoothness and continuity of the transition between branches of space-time;
- Analysis of the influence of mirror symmetry on the geometry of the metric and particle dynamics.

The concept of mirror symmetry, used in string theory and other areas of theoretical physics, suggests interesting parallels with our hypothesis, allowing us to assume its applicability in other aspects of physics, including the limits of the speed of light [26, 27].

Prospects and Experimental Opportunities

The proposed model may open new avenues for understanding extreme physical states, including.

Analysis of particle motion at speeds close to the speed of light, with the possibility of exceeding the classical limit.

- Analysis of particle motion at speeds close to the speed of light, with the possibility of exceeding the classical limit.
- Studies of anomalies in the motion of objects near black holes and other strong gravitational fields.
- Potential for experimental verification through high-energy experiments and astronomical observations.

An interesting point is the speed $v = \frac{c}{\sqrt{2}} \approx 0{,}707c$, which may play a key role in mirror symmetry [28]. Reaching this speed could trigger significant effects, potentially linked to the existence of a mirror world. Experimental data on particle behavior at this speed might reveal anomalies, pointing to new physical phenomena and supporting the hypothesis of mirror symmetry in space-time.

Confirming or refuting this study through simple astronomical observations will be difficult, since φ = 1° in such a geometry could correspond to billions of years in our real space. Because of this, there is a possibility of errors in interpretation and conclusions.

For example, it is known that the Earth's rotation around its axis is gradually slowing down. This phenomenon can be associated with time dilation in the Earth's gravitational field. Although we do not notice it directly with clocks, the slowing of the Earth's rotation around its axis is quite evident.

Such a geometry predicts that the Earth's radius should also gradually decrease. We do indeed

observe these changes: the Earth's rotation speed is decreasing, and tectonic shifts, earthquakes, and volcanoes confirm similar processes.

However, a logical contradiction arises when we consider that, according to this geometry, the Moon should be approaching the Earth [29]. In practice, modern data show that the Moon is moving away from the Earth. This phenomenon is primarily explained by the tidal forces acting between the Earth and the Moon [30].

This process has been observed for millions of years and may continue for billions of years. The effect of this process on the distance between the Earth and the Moon is currently recorded through scientific observations.

If we attempt to predict what will happen in a billion years, unexpected outcomes may arise due to changes in the gravitational field or climate. The Earth's oceans could be altered by these factors, potentially leading to their reduction or even complete evaporation.

Under such conditions, how would this affect the distance to the Moon? Would the Moon continue to recede, or, on the contrary, begin to approach the Earth?

Since it is impossible to observe billions of years in reality, the question remains open. However, taking such a geometry into account, it is possible to attempt to forecast the overall development and determine which processes will dominate. Should we expect the current trend of the Moon’s recession to continue, or does such a space-time geometry predict a different outcome?

Although on short time scales we may observe unpredictable behavior that does not align with the geometry and somewhat resembles chaos, over long periods, such effects can become ordered. This ordering occurs due to relativistic laws and gravitational effects. This makes the model more coherent, allowing it to explain not only current discrepancies in the process but also long-term developmental trends.

However, in the case of ordinary astronomical objects that still follow Newtonian laws, confirming the hypothesis will be difficult, as data for such objects will mostly align with existing models. The best data for testing the hypothesis could be obtained by studying the behavior of astronomical objects in conditions of strong gravitational fields and exotic space-time structures.

Computer visualization of matter motion in such a geometry provides a clear illustrative effect. Figure 7 shows a study of the dynamics of material points near a black hole using computer visualization. According to the structure of the metric, all matter moves toward the center of the black hole, regardless of the observer.

In the proposed geometry, the motion of matter near a black hole depends on the observer's frame of reference:

• For a distant observer (in a weak gravitational field), matter falls into the black hole with acceleration, as in classical General Relativity.

• For a local observer (for example, near the event horizon), the motion of matter gradually slows down, and its velocity approaches zero. This is because the angle ϕ provides a smooth transition between relativistic and gravitational effects, eliminating divergences in the metric.

Thus, the model unifies both descriptions, offering a more comprehensive understanding of dynamics under extreme conditions.

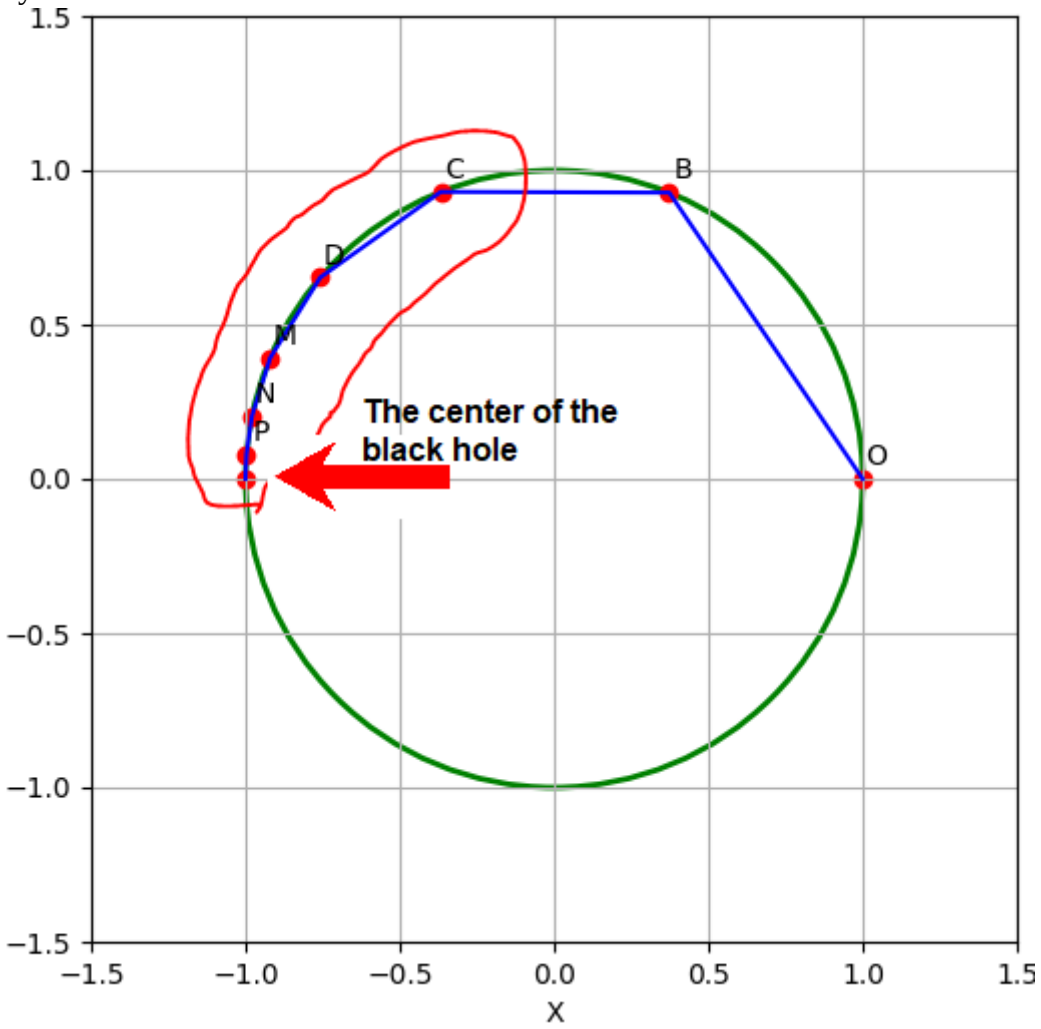

Figure 7 — *Visualization of matter dynamics around a black hole using computer graphics*

This approach allows for a visual assessment of the influence of the metric on the dynamics of matter and highlights how coordinate dependence alters the perception of motion and time.

Such objects include black holes, neutron stars, and systems with strong tidal forces. In these conditions, space-time exhibits more extreme and noticeable deviations, providing the opportunity to observe phenomena that cannot be explained by classical Newtonian laws.

Despite the challenges, the proposed geometry can be experimentally tested through a carefully planned experiment. As an example, one could consider a modification of the classical Cavendish experiment. Modern high-precision measuring instruments would be capable of detecting both masses and local variations in the flow of time.

Particle Energy and Local Gravitational Effects

The classic Cavendish experiment (1797–1798) was the first to measure the gravitational attraction between massive bodies and determine the gravitational constant G. In the original setup, the masses were stationary, and attention was focused solely on the static effect of gravitational force.

The proposed variant represents a modern extension. In this version, one of the masses rotates at high speed, creating a local change in kinetic energy and, consequently, a possible influence on the spacetime metric. This allows not only measuring the change in gravitational attraction but also assessing the impact of the mass's motion on the local flow of time.

Thus, the experiment combines classical measurement of gravitational force with new aspects:

• testing the influence of kinetic energy on the gravitational field;

• studying local time deviations around a rotating mass;

• directly testing the hypothesis of the connection between kinematics and gravity within the framework of the proposed geometric model.

This makes the experiment not merely a repetition of Cavendish's work. It becomes a unique opportunity to investigate new fundamental effects in laboratory conditions using modern high-precision instruments.

In addition to mass rotation, a separate experiment can be considered in which one of the large masses is heated to a high temperature. According to the proposed geometric model, high thermal energy corresponds to weaker gravitational interactions, while as the temperature decreases, the gravitational force increases.

The modified experiment involves:

• placing one of the large masses in a heater with controlled temperature;

• measuring the gravitational force between the hot and cold masses;

• measuring local time deviations around the hot and cold masses.

It is expected that at high temperatures, gravitational attraction will be weakened, and local time deviations will be reduced. This experiment allows a direct test of the influence of thermal energy on the local spacetime metric. It further expands the possibilities for testing the proposed geometric model.

The two experiments, although different in mechanics (rotation and heating of a mass), together provide a comprehensive test of the hypothesis regarding the influence of a system's energy (kinetic and thermal) on gravity and the flow of time within the proposed model.

This could become the first step toward testing such a geometry.

13. Mirror Symmetry and Matter Transition in Extreme Conditions

In the proposed geometric model, electrons of superheavy elements approach the speed of light, indicating a phase transition of matter toward a state close to singularity. When electrons move at extremely high velocities, possibly near the speed of light, this becomes part of a larger physical transformation—a transition toward singularity.

This can be compared to the picture of a black hole. One could say that matter falls at near-light speed. From a mirror perspective, it can be argued that the falling velocity in a black hole does

not increase indefinitely. Instead, it gradually approaches the speed of light. Conversely, with mirror symmetry, one can assert that the velocity gradually approaches zero.

A similar process can be envisioned for the behavior of an electron in an atom when extreme events occur near singularities. In this context, the transition from “moving” matter to “resting” matter in mirror space represents the final stage. At this stage, all particles—including electrons and nuclei—converge into a single state. This state is more stable, yet physically transformed.

This supports the idea that matter can be viewed as undergoing a phase transition between two states—active motion and rest. This transition leads to the formation of a new state of matter. This state may exist potentially at the boundary of a singularity [31, 32].

Mirror symmetry in the context of the atom can be interpreted as the relationship between high-energy states (in our space) and rest states (in the mirror space). For example, consider an atom as a system with a nucleus and electrons. These electrons can reach a state where their energy tends toward infinity. Conversely, they can slow down in the mirror space. This provides a way to describe such a transition.

Relativistic Corrections to the Atomic Model:

For atoms, relativistic corrections can be expressed through a modification of the Schrödinger equation (28) for the electron’s energy:

$$E_{rel} = -\frac{K}{n^2} \cdot \frac{1}{\sqrt{1-\frac{v^2}{c^2}}} = -\frac{K}{n^2} \cdot \frac{1}{\cos(\varphi)} \quad (28)$$

where v is the electron velocity, c is the speed of light, K is a constant depending on the nuclear charge, and n is the principal quantum number [33, 34]. This equation demonstrates how a velocity approaching the speed of light affects the energy of the atom. As the velocity approaches c, the energy tends toward infinity, but in mirror space, this energy tends toward zero, illustrating a phase transition between these states. Through mirror symmetry, the motion of the electron in our world with v→c corresponds to a state of rest in the mirror world with v′=0, which yields a finite energy and eliminates the singularity. The parameter φ allows for a smooth transition from ordinary energy to the limiting energy, avoiding singularity. Mirror symmetry is a geometric tool that allows one to "translate" extreme values into a manageable, finite form.

Mirror symmetry can also be used to explain the behavior of atoms under extreme conditions, such as at high energies. In mirror space, electrons moving at high velocities transition to a state of rest, which is associated with a phase transition of matter. This explanation can be supported through the Schrödinger equation or relativistic corrections, adapted to account for mirror symmetry, providing a deeper understanding of atomic behavior under such conditions.

Thus, mirror symmetry not only eliminates singularities but also visualizes the transitions of matter and energy, revealing a deep connection between the quantum states of the electron and the geometry of space-time.

Phase Transition at the Atomic Scale

- Under ordinary conditions, the atomic model:
- The electron moves with v≪c → the classical relativistic correction is small.
- At extreme energies (close to the speed of light), conventional Special Relativity predicts an energy singularity.

Through mirror symmetry:

- An electron in our world with v→c↔ an electron in the mirror world with v′=0
- The energy remains finite; the singularity disappears
- A phase transition of matter arises: motion ↔ rest, infinite energy ↔ finite energy.

Thus, the quantum state of the electron is linked to the geometry of space-time, and mirror symmetry allows visualizing and describing the behavior of atoms under extreme conditions.

Intuitive Formula via Mirror Symmetry:

$$E_{Our\ world} \sim \frac{1}{\cos(\varphi)}, E_{Mirror\ World} \sim \cos(\varphi), v \to c \iff E_{Our\ world} \to \infty, E_{Mirror\ World} \to 0$$

That is, one value increases, another decreases - as in a phase transition.

14. Gravitational Consistency, Global Structure, and Symmetric Antimatter

In the proposed geometric model of the Universe, the gravitational constant G retains its fundamental significance at all scales [1]. Different structures—planets, galaxies, and clusters—may collapse at varying rates and with local accelerations. However, all dynamics are coordinated through a unified metric.

This ensures the universality of G and the harmony of the system. Even along different trajectories, the motion of matter is governed by a single space-time structure. The speed of light c, mass M, and the gravitational constant

G remain a key quantity determining the behavior of matter, both in the Schwarzschild equation and in the overall geometry of the model [5].

Points E and O represent global singularities [35], toward which all matter—and, so to speak, antimatter—moves along individual trajectories defined by the metric. Their existence confirms the consistency of the model and the relativistic addition of velocities [12].

Antimatter and Symmetric Metric

The observed near-complete absence of antimatter in our metric can be explained by assuming the existence of a symmetric metric. In this metric, matter and antimatter are distributed mirror-like relative to our Universe. In this scenario:

- Antimatter is concentrated in the "other metric" and practically does not interact with our own.
- An observer in our metric predominantly sees matter, which corresponds to experimental observations.
- The search for antimatter on Earth and in space serves as a test: whether this symmetry exists and whether traces of transitions or interactions between the metrics can be observed.

Thus, the hypothesis of a symmetric metric provides a logical explanation for the antimatter deficit and can become a testable proposition within the framework of modern physics.

Conclusion

- The speed of light and zero velocity represent the same state of an object, observed through different metrics.
- The energy is always finite; there is no critical singularity.
- Gravitational consistency ensures a single metric for all matter.
- The speed of light limit becomes a phase transition rather than an unattainable boundary.
- A symmetric metric with antimatter explains the observed deficit of antimatter and the consistency of time between the metrics.

15. Eccentricity and orbital velocities through the angles Φ_p, Φ_a: testing on planets

In this paragraph, we consider an example of a method for calculating the eccentricity and orbital velocities of planets through the angles Φ_p and Φ_a, corresponding to the planet's positions at perihelion and aphelion [36]. This approach is a verification method based on the assumptions of the geometric model. The method allows one to calculate the eccentricity and velocities without directly using the minimum and maximum orbital radii (r_p and r_a), relying instead on the angles Φ_p and Φ_a corresponding to the planet's positions at perihelion and aphelion.

Logical Basis of the Calculation Method

Let us assume that a planet moves along an elliptical orbit. Its position at perihelion is defined by the angle Φ_p, and at aphelion by the angle Φ_a. These angles are derived from the geometric model, where radii and velocities are connected through trigonometric functions, similarly to symmetric coordinate metrics.

Using symmetry, the relationships between radii and velocities can be expressed through the angle functions, which then allows calculating the eccentricity e and the orbital velocities.

Formulas for Calculating Radii, Eccentricity, and Velocities

Let $S(\Phi)$ and $T(\Phi)$ be functions representing the radial coordinates in the chosen metric:

$S(\Phi) = R_0 \cdot \cos(\Phi)$ (29)
$T(\Phi) = R_0 \cdot \sin(\Phi)$ (30)
where R_0 is the scale radius, defining the characteristic size of the model.

$S(\Phi)$ is intended to be used to calculate the radii at perihelion and aphelion: $r_p = S(\Phi_p),\ r_a = S(\Phi_a)$. That is, formally, it can be written as: $\Phi_p = arccos\left(\frac{r_p}{R_0}\right)$ (31), $\Phi_a = arccos\left(\frac{r_a}{R_0}\right)$ (32).
The function $T(\Phi)$ can be considered as a mirror reflection of $S(\Phi)$: if one observer measures the radius using $S(\Phi)$, another "looks through the mirror" and sees the corresponding value of $T(\Phi)$. Alternatively, $T(\Phi)$ can be interpreted as the projection of the radius from a different perspective, for example, from above or below the orbit. This approach allows one to consider symmetric branches of orbital dependencies and facilitates the visualization of the planet's motion relative

to different observers.

The angles Φ_p and Φ_a in the model can be interpreted as parameters reflecting the deviation of the orbit's radii from the average "ideal" circular radius. In simpler terms, these angles indicate how much the planet's position at perihelion or aphelion deviates from the mean orbital circle, providing a geometric basis for calculating the eccentricity and orbital velocities.

The eccentricity can be defined as: $e = \frac{r_a - r_p}{r_a + r_p}$ (33).
Orbital velocities (using a formula analogous to the law of energy conservation):
$v_p = \sqrt{GM\left(\frac{2}{r_p} - \frac{1}{a}\right)}$ (34), $v_a = \sqrt{GM\left(\frac{2}{r_a} - \frac{1}{a}\right)}$ (35), $a = \frac{r_p + p_a}{2}$ (36)
Example calculation for Mercury:
1. For Mercury, according to the geometric model, we obtain:
   $\Phi_p = 40.12°$
   $\Phi_a = 49.88°$
2. Radii:
   r_p = R₀· cos(40.12°) = 46.0 million km
   r_a = R₀·cos(49.88°) = 69.8 million km
3. Eccentricity:

$$e = \frac{(69.8 - 46.0)}{(69.8 + 46.0)} \approx 0.2056$$

Observed value: 0.2056 (error ≈ 0.0%).
Velocities: $v_p \approx 58.98$ km/s, $v_a \approx 38.86$ km/s .
Observed values: 58.98 km/s, 38.86 km/s (error ≈ 0%).

Planet	Φ_p (°)	Φ_a (°)	e (calcul)	e (obser.)	error. ≈ (%)
Mercury	40.12	49.88	0.2056	0.2056	0.0
Venus	44.94	45.06	0.0068	0.0068	0.0
Earth	44.99	45.01	0.0167	0.0167	0.0
Mars	43.41	46.59	0.0934	0.0934	0.0

Table 7 — *Comparison for several planets*

Conclusion:

The method based on the use of angles Φ_p and Φ_a, allows for accurate determination of planetary eccentricities and orbital velocities without directly measuring $r_p$and r_a. The errors Table 7 for the tested planets were practically zero, confirming the validity of the approach and its underlying geometric model.

16. Historical Problem of Computational Instability and the Role of the Angular Method Φ

This paragraph discusses the historical problem of computational instability when working with trigonometric formulas in electrodynamics, astronomy, and related fields.

It then demonstrates how the angular symmetry method (the Φ method) addresses these difficulties.

This method preserves the physical interpretation while improving the stability of calculations.

1. Historical problems

Before the advent of modern double-precision computing systems, engineers and physicists faced significant difficulties. This was especially pronounced when performing calculations for angles close to 0° or 90°. For example, when computing light reflection parameters, critical angles in optics, or orbital characteristics in celestial mechanics, the value of cos(θ) could become very small. This can lead to the loss of significant digits, a problem known as the subtraction catastrophe.

This led to large relative errors in calculations, particularly when cos(θ) was on the order of 10^{-6} or smaller. In such cases, complex analytical transformations of formulas were required to avoid division by very small numbers.

2. Lack of universal techniques

Another problem was the absence of a universal approach that would allow formulas to be rewritten simply and clearly for numerical stability. Usually, either approximations or separate value tables were used. For example, in geodetic astronomy, practitioners would manually switch to the "complementary" angle to replace a small cos(θ) with sin(90°−θ), but this required additional justification and was not always applied systematically.

3. Current situation

With the development of computing technology, including double and extended precision, the problem of overflows and loss of significance has been greatly reduced.

The emergence of mathematical software packages, such as Mathematica, Matlab, and NumPy, has also helped to nearly eliminate these issues. However, at extreme angles, numerical errors are still possible.

4. Role of the Φ Method

The angular symmetry method (Φ method) offers a geometric way to transform expressions so that formulas automatically switch to a stable branch—cosine or sine, depending on the situation.

This:

1) Increases the numerical stability of calculations.

2) Provides a physical interpretation through symmetry: replacing cos with sin via Φ reflects the mirrored branch of the angle, corresponding to a numerically and physically stable state.

3) Is universal—applicable in celestial mechanics, electrodynamics, optics, and other fields.

5. Historical Example

Consider the problem of calculating the reflection coefficient at an incidence angle of 89.999°. In the classical approach, $\cos(\theta) \approx 1.745\times10^{-5}$, which leads to division by a very small number and unstable results. Using the Φ method and switching to the complementary angle (90°−θ), we replace cos(θ) with sin(Φ), which in this case is close to 1, ensuring a stable and reliable result.

Fresnel formulas and branch replacement

When an electromagnetic wave strikes the boundary between two media with refractive indices $n1$ and $n2$, the angle of incidence θ and the angle of refraction θ_2 are related by Snell's law:
$n_1 \sin\theta = n_2 \sin\theta_2$ (37).
Reflection amplitudes for TE and TM polarizations (Fresnel formulas) [37–41]:

$$rTE = \frac{(n_1 cos\theta - n_2 cos\theta_2)}{(n_1 cos\theta + n_2 cos\theta_2)} \quad (38)$$

$$rTM = \frac{(n_2 cos\theta - n_1 cos\theta_2)}{(n_2 cos\theta + n_1 cos\theta_2)} \quad (39)$$

$$R = |r|^2 \qquad (40)$$

The Φ method is naturally applicable to these formulas and allows for a clear selection of stable branches:
- For TE: cos θ → sin Φ (sin- branch);
- For TM: 1/cos θ → 1/sin Φ (mirror cos branch).

The Φ method allows one to “see” the system’s mirror behavior: one observer perceives the process from above, while another sees it from below; the sine and cosine branches reflect these alternative points of view. Thus, the transition between branches acquires a physical meaning rather than remaining a purely mathematical operation (see Figure 1: view inside the triangle from point O and view inside the triangle from point E). Now the physical significance of the method is clearly visible.

Advantages of the Φ method:

1. Numerical stability near θ ≈ 90°;
2. Physical clarity of transitions between regimes;
3. Universality of the approach—applicable in electrodynamics, mechanics, and astrodynamics.

Conclusion:

Historically, computational instability when working with small values of cos(θ) and sin(θ) posed a serious problem and required special methods. The Φ method can serve as a universal solution in such cases, allowing not only the stabilization of calculations but also the preservation of the physical clarity of processes. It neatly organizes the branches of the formulas and makes the transitions between them intuitively clear, without violating the physical meaning, which is especially valuable in complex calculations.

17. Potential Application Areas and Examples of the Angular Method Φ

The Φ method—mirror-symmetric calculations (replacing the original angle θ with the complementary angle Φ = 90° − θ, splitting the formulas into two mirror-symmetric branches:

the sin-branch and the cos-branch)—helps to avoid numerical instability near "problematic" angles, where the original formulas contain factors $\cos\theta \to 0$ or $\sin\theta \to 0$.

If we consider the kinematic expression $\sqrt{1-\frac{v^2}{c^2}}$ and the gravitational expression $\sqrt{1-\frac{2GM}{rc^2}}$, they can be interpreted as functions analogous to sine and cosine, depending on the observation point. In other words, visualizing these quantities through the chosen observational metric reveals periodic, sinusoidal, and cosinusoidal patterns (see Figure 8).

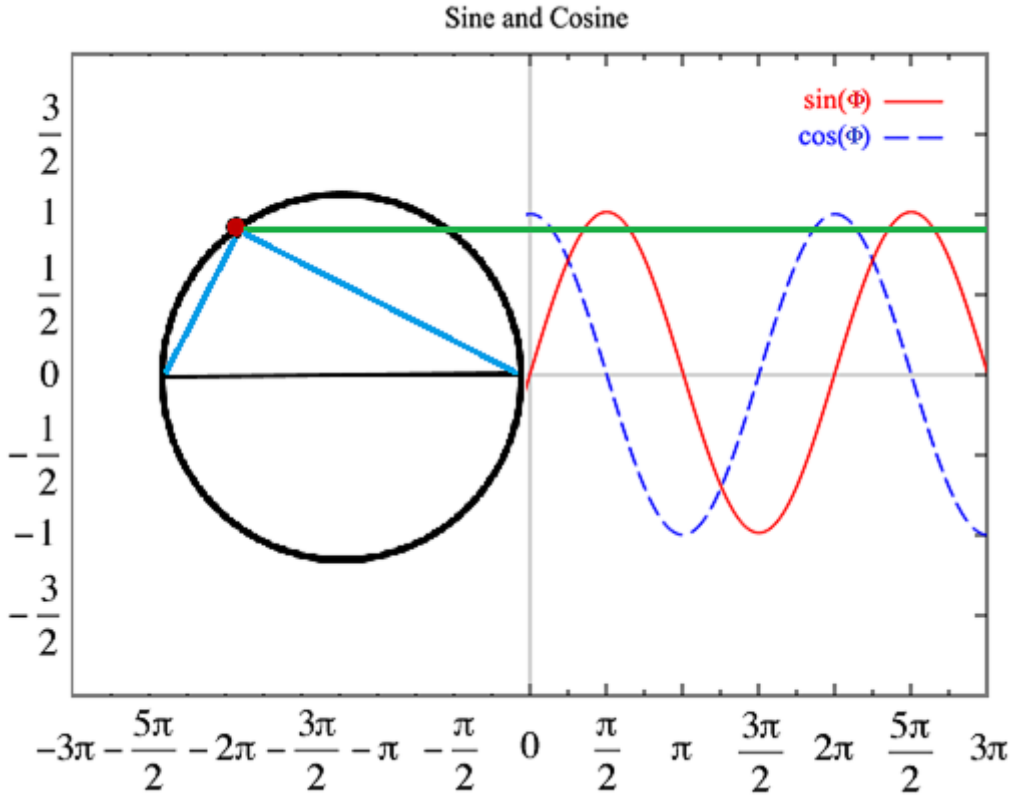

Figure 8 — *sinusoidal and cosinusoidal relationships*

As an example, let us rewrite the formula for relativistic velocity addition (1) in the form of a trigonometric function.

As shown in Figure 2, the velocities can be expressed using trigonometric functions: $v(OA) = c \cdot \sin(\varphi_1),\ v(AB) = c \cdot \sin(\varphi_2)$.
Substituting these expressions into the formula for relativistic velocity addition, we obtain:

$$v(OB) = \frac{v(OA) + v(AB)}{1 + \frac{c \cdot \sin(\varphi_1) \cdot c \cdot \sin(\varphi_2)}{c^2}} \Leftrightarrow v(OB) = \frac{c \cdot (\sin(\varphi_1) + \sin(\varphi_2))}{1 + (\sin(\varphi_1) \cdot \sin(\varphi_2))} \quad (41)$$

The proposed analysis demonstrates a key feature of relativistic velocity addition. It highlights the relationship between the limiting states v→0 and v→c. Equation (41), together with Figure 8, vividly illustrates this connection. It shows how the velocities of objects in different reference frames conform to the fundamental limits of relativistic dynamics.

In this relativistic expression, rewritten in terms of trigonometric functions, the relationship between the limiting states v→0 and v→c is clearly illustrated, showing that they represent two aspects of the same underlying dynamical pattern in relativistic mechanics.

This representation is applicable both to macroscopic systems and to particles of the microscopic world, and it can also serve as a tool for analyzing relative velocities in other areas of physics. At the same time, a complete demonstration of all consequences of the proposed model requires collaborative mathematical and experimental work.

The present article is intended to provide a conceptual foundation and a visual interpretation, which may stimulate further research and verification of the model by other specialists.

Fundamental physical expressions, such as:

$$\gamma = \frac{1}{\sqrt{1-\frac{v^2}{c^2}}}, \sqrt{1-\frac{2GM}{rc^2}}$$

can be interpreted as functions analogous to sine and cosine, depending on the observation point. Visualization of these quantities through the chosen observational metric reveals periodic, sinusoidal, and cosinusoidal patterns (see Fig. 8).

This transformation retains its form regardless of the system scale. In principle, it can be applied both to macroscopic bodies and to microscopic particles. It may also be utilized in other areas of physics. For example, it can help analyze relative velocities and the dynamics of moving objects.

Thus, the proposed spatial geometry allows complex relativistic dependencies to be transformed. These dependencies take a form convenient for visualization and calculations. Essentially, they are reduced to trigonometric functions. This simplifies the analysis of the dynamics of material points. It enables an intuitive understanding of the interplay between kinematics and gravity. This is achieved through sinusoidal and cosinusoidal relationships.

Such approaches are especially useful when analyzing extreme states of physical systems, where standard equations lose accuracy—for example:

Singularities in General Relativity

Problem: At singular points (the center of a black hole, the moment of the Big Bang T→0), the standard Einstein equations yield infinite values of curvature and density.

Difficulty: The classical Schwarzschild metric cannot describe the behavior of matter at these points, leading to numerical divergences and a loss of physical meaning.

Connection to the Φ method: Using mirror symmetry and complementary angles allows one to parametrize fields and the metric near the singularity without resorting to “infinite” quantities.

Critical states at relativistic speeds

Problem: At velocities close to the speed of light, many relativistic formulas (γ-factor, momentum, energy) become numerically stiff:

$$\gamma = \frac{1}{\sqrt{1-\frac{v^2}{c^2}}}$$

As v→c, the denominator →0, leading to both computational and conceptual difficulties.

Challenge: Analysis of particles and fields in accelerators, modeling relativistic flows, especially in matter–antimatter interactions.

Connection to the Φ method: Switching to the complementary angle or function branch allows "unfolding" the numerically dangerous expression, preserving both physical meaning and computational stability.

Cosmological extreme conditions (early Universe)

Problem: The moment of inflation and the initial conditions of the Big Bang ($T \to 0$), when densities and curvatures become extremely high and standard variables are poorly defined.

Challenge: Traditional numerical methods yield chaotic or divergent results.

Connection to the Φ method: Symmetric reparameterization allows "smoothing" the functions of density, temperature, and curvature, making plots and calculations more predictable.

Caustics and critical angles in gravitational lensing astronomy

Problem: Light passing through strong gravitational fields forms caustic lines and singular points, where standard methods for calculating intensity and refraction angles produce uncertainties.

Connection to the Φ method: Replacing angles with complementary branches stabilizes calculations, making the visualization of the light field smooth and clear.

The problem of "zero velocity" and the "matter–antimatter transition"

Problem: There is no unified formalism for extreme transitions where matter formally slows down to zero and can convert into antimatter.

Connection to the Φ method: The method provides a stable numerical and conceptual interpretation of such processes, even at a purely theoretical level.

Below, as an example, is a list of areas where such a substitution can simplify calculations, increase the stability of formulas, and make boundary behavior more visually clear.

Optics and Photonics

- Fresnel formulas (TE/TM) at large angles of incidence [37–41].
- Brewster's angle (stable estimation of the TM minimum).
- Total internal reflection (stable calculation of $R \to 1$).
- Multilayer coatings and interference filters under oblique incidence.

Electrodynamics and Antennas

- Calculation of radiation patterns at angles close to the horizon [42, 43].
- Waveguide modes under critical conditions [44, 45].
- Scattering and diffraction on slits at large angles [46, 47].

Astronomy and Celestial Mechanics

- Atmospheric refraction [48].
- Dispersion and deviation of spectra in prisms/gratings [49].
- Aberrations and diffraction.

- Calculation of the field of view and image scale.
- Interferometric spectrographs.
- Computation of orbital velocities and eccentricity without directly using distances.
- Planetary photometry at phase angles close to 0° or 180° [50].
- Light scattering on dust (Henyey–Greenstein law) at boundary angles.
- Stable parameterization near caustics [51].

Preliminary studies on the application of stable parameterization near caustics have shown promising results. Initial calculations using the replacement of functions, such as cos → sin and vice versa, demonstrate clear advantages. Computational procedures become simpler, more stable, and more predictable. They also become easier to interpret visually. Previously chaotic graphs acquire a smooth and clear character, facilitating data interpretation.

At the same time, this problem is highly sensitive and methodologically complex. Therefore, enhanced attention is required at all stages of development. Involvement of domain experts is also essential for proper verification. This is necessary to ensure the correctness of conclusions and the reliability of the proposed methodology.

Such stable reparameterization can be integrated into computational algorithms and software. When encountering “problematic” values, standard formulas may lose accuracy. In such cases, the system can automatically apply angle or function replacement, similar to the Φ method. It can then check how much the calculations improve in stability. This would not only speed up data processing but also reduce the likelihood of numerical artifacts, providing correct and reproducible results almost “on the fly“.

Thus, the method acquires practical value, becoming not merely a mathematical trick but a physically reproducible approach. This approach reinforces our geometric understanding and can serve as a practical tool for solving a wide range of problems in optics, astronomy, geodesy, and other fields.

Geodesy and Satellite Navigation

- Conversion from elevation angle to zenith angle in tropospheric corrections [52].
- Map projections (stereographic and others) near the poles [53].
- Ray tracing for nearly horizontal propagation through the atmosphere [54].

Classical and Quantum Mechanics

- Particle scattering (Rutherford, Mie formulas) at small and large angles [55].
- Moments of inertia of bodies with inclined axes — conversion to a stable form [56].
- Tunneling models at small transverse momenta [57].

Numerical Analysis and Computational Mathematics

- Legendre functions and spherical harmonics as $|x| \to 1$ [58].
- Solving wave equations at large Fresnel numbers [59].
- Asymptotic expansions in geometric optics and acoustics [60].

Situation	Problem	Application of Φ Method
Singularities in General Relativity (e.g., black hole center, T→0)	Density and curvature → ∞	Field parametrization using Φ allows avoiding "infinities"
Relativistic speeds (v→c)	γ → ∞, numerical instability	Switching to complementary angle stabilizes calculations
Early Universe conditions	Extremely high density, temperature, and curvature	Provides stable graphical and numerical representation
Caustics in gravitational lensing	Undefined refraction angles	Replacing angles with Φ makes calculations smooth
Matter ↔ Antimatter transition	No formalism for critical-speed transitions	Φ method provides numerical and conceptual interpretation

Table 8—*Applications of the Φ Method in Critical Physical Situations*

Note:

Some specific examples of situations and corresponding advantages of the Φ method are summarized in Table 8.

The proposed methodology requires further verification and adaptation by specialists in the relevant fields, while the underlying ideas and general approach are described in this work. Each case requires individual validation, and due to the volume of tasks, it is practical to carry this out as part of a collaborative effort. This strategy will enable researchers to identify areas where the method offers genuine advantages and where modifications or abandonment of its use may be necessary.

In cases where equations involve trigonometric functions and computational difficulties arise, it is advisable to test the proposed method. In the absence of explicit trigonometric expressions, the approach can be adapted—analogously to our application in problems related to velocity and the speed of light. The method appears particularly promising in situations where the equation contains a Lorentzian or Schwarzschild-type radical, as such a structure directly suggests the possibility of stable reparameterization.

Our geometry (see Figure 1), based on symmetry, allows us to switch branches of trigonometric functions: in complex situations, sines can be replaced with cosines. Visually, this can be represented as follows: if difficulties arise in calculations relative to point O, computations can be temporarily transferred to point E to obtain smooth solutions. After simplifying the numerical calculations, one can, based on the principle of symmetry, analyze what exactly occurs at the original point O.

This approach may serve as a practical tool. It allows one to move from uncertain and distorted results to accurate and reproducible conclusions. In doing so, it opens new perspectives for testing fundamental hypotheses. In the future, if the method proves advantageous in numerical

calculations of extreme states, its application could stimulate experimental verification. For instance, colliders could be used to monitor critical energy- or mass-limited states. This would provide a direct test of theoretical predictions.

Thus, the proposed method can serve as a guide in choosing stable approaches under conditions of uncertain input data and numerical difficulties.

18. Critical speed $\frac{c}{\sqrt{2}}$ and mirror symmetry in the expansion of the Universe

According to the proposed geometric model, in the initial phase of the Universe's expansion after the Big Bang, material points begin to move away from each other. One of these points can be considered as a conventionally stationary frame of reference, relative to which the other points exhibit divergence.

As the distances between points increase, a moment occurs when the relative velocities in the transverse direction reach or exceed the critical value $v=c\cdot\sin(45^\circ)=c/2\approx 0.707c$. In Figure 9, this moment corresponds to the position of point K, where the expansion velocity relative to the conventional stationary point O reaches the specified critical threshold.

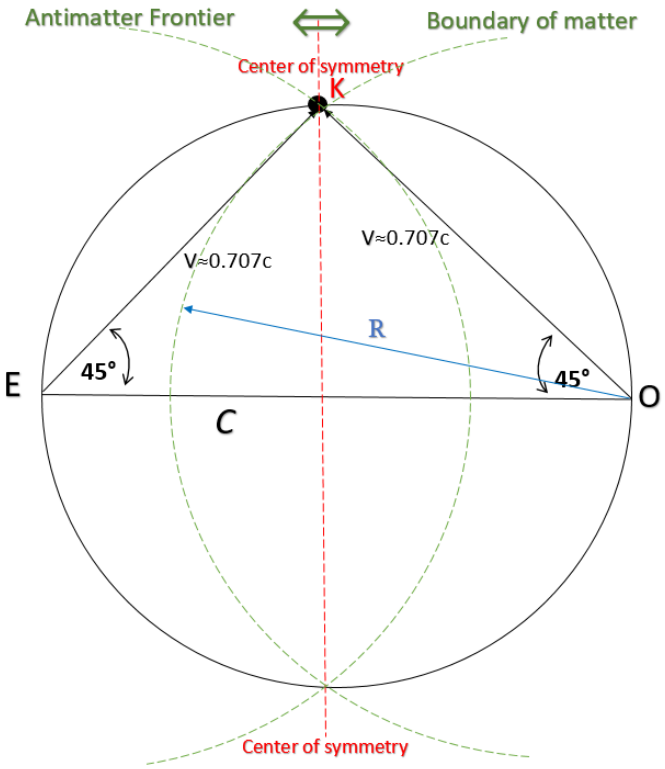

Figure 9 — *Illustration of Mirror Symmetry*

It should be emphasized that, in this geometry, immediately after the so-called Big Bang, the Universe was in a state of extremely high temperature. At the same time, fundamental physical parameters — such as mass, the gravitational constant, and other characteristics — were already present at the initial moment. However, the gravitational forces themselves remained weakly expressed.

According to the findings of Kahniashvili and Machabeli (1997) [61], as well as Chicone and Mashhoon (2004) [62], reaching a critical speed leads to a change in the sign of the centrifugal acceleration, which qualitatively alters the dynamics of particle motion and the distribution of forces in space. Within the framework of this geometry, this implies that the centrifugal force, which previously resisted the compression of matter, instead begins to facilitate its gravitational localization.

This transitional moment can be considered as a triggering mechanism for the formation of stellar and planetary systems: local density fluctuations that fall within the region of this transition begin to collapse under the influence of the increasing gravitational attraction.

Thus, the critical speed c/2 acquires fundamental significance not only in relativistic mechanics but also in cosmogenesis. It serves as a threshold state between diffuse expansion and the localized formation of structures.

According to the proposed geometry, at speeds around $v=c\cdot\sin(45^{\circ})=c/2\approx 0.707c$, anomalous effects may be observed. This prediction illustrates that the model is capable of revealing new physical states that the classical Schwarzschild metric only qualitatively addresses, and it requires experimental verification.

Beyond point K, matter continues to move toward the event horizon: for one observer, toward point E; for another, toward point O. The overall trend of expansion or contraction is preserved, but the internal structure of the metric becomes narrower and denser.

The presence of point K plays a key role, dividing space into two symmetric regions.

Point K, where the speed approaches c/2, symbolizes a splitting point in the space-time structure. This can be interpreted as the moment when space separates into two states, in which the dynamics of matter change depending on the speed approaching the speed of light. On one hand, in our space, the speed increases; on the other hand, in the mirror space, the speed tends toward zero, indicating a transition of matter to a state of rest.

Examining these processes through the lens of mirror symmetry provides new ways to understand gravity and cosmogenesis.

In this framework, objects can move between states, passing through a phase transition between active and passive states of matter.

The concept of critical speed and mirror symmetry offers a new perspective on the dynamics of the Universe's expansion. It also sheds light on the formation of cosmic structures, creating promising avenues for further research.

19. Geometry as a Bridge Between Relativistic Dynamics and Other Areas of Physics

The unification of general relativity and electromagnetism was Einstein’s dream, and our method demonstrates a possible first step toward this goal by introducing a geometric parameterization via the angle φ:

$$v = c \cdot \sin(\varphi), \qquad \gamma = \frac{1}{\cos(\varphi)}$$

We relate the limiting behavior of the speed of light in relativistic mechanics to the mutual transformation of electric and magnetic fields. The Lorentz transformations for the transverse

components of the fields take the form:

$$E'_{\perp} = \frac{1}{\cos(\varphi)}(E_{\perp} + csin(\varphi) \cdot \hat{v} \times B) \quad (41)$$

$$B'_{\perp} = \frac{1}{\cos(\varphi)}\left(B_{\perp} - \frac{\sin(\varphi)}{c}\hat{v} \times E\right) (42)$$

In this formulation, the 'switching' of electric and magnetic components becomes visual as φ → 90°, that is, in the limit v → c. What appears as a formal singularity (γ → ∞) in the standard scheme is naturally interpreted in our geometry as a phase transition: the electric field partially transforms into the magnetic field, and vice versa.
Fundamental Lorentz invariants:
$I_1 = E^2 - c^2B^2, \quad I_2 = E \cdot B$

are preserved, confirming that the mirror symmetry does not violate the consistency of electromagnetic theo
− of − light limit with the interconversion of electric and magnetic fields.

Thus, mirror symmetry functions not only as a way to remove the singularity in the limit v→c, but also as a tool for describing the phase transition "motion ↔ rest" in mechanics and "electric ↔ magnetic component" in electrodynamics. The same geometric principle ϕ links relativistic dynamics and electromagnetic fields, demonstrating their unified "mirror" structure.

The next step should involve a deeper investigation of this phase transition and an examination of potential physical manifestations of this connection. We do not claim to provide a complete solution to the problem posed by Einstein. However, we propose a possible bridge.

This bridge could serve as a foundation for future studies. It may also enable a more thorough test of the unity between relativistic dynamics and electromagnetism.

Analogous to the connection between relativistic dynamics and electromagnetism via the ϕ - parameter, the idea of mirror symmetry can be extended to quantum and string physics. In quantum theory, ϕ could describe smooth transitions between quantum states, while in string theory, it may link different vibrational modes and mirror Calabi–Yau spaces. Furthermore, applying mirror geometry in quantum physics could help smooth extreme transitions between states. It may also simplify calculations in limiting cases, where standard methods often produce "jumps" or singularities. Thus, this geometric approach could serve as a bridge between classical and modern theories, opening a pathway for further exploration and testing the unity of physical laws across different scales.

20. Critical State v=c=0 and Its Testability

Yes, the term v=c=0 is unusual, and it is not an ordinary equality of velocities, but a symmetric state of threshold dynamics, where in one branch v→0, and in the other v→c.

In the proposed mirror-symmetric geometry, a key role is played by the critical state v=c=0, which is not an arbitrary hypothesis but follows from the relativistic addition of velocities. The physical meaning of this state can be interpreted as a threshold:

- v→0 — a particle or a point in space-time is effectively “frozen” relative to an observer in the mirror system;
- v→c — a limiting relativistic state is reached, in which the classical constraints of mechanics no longer apply.

Together, these conditions form a kind of “stratification point”, where the diffuse expansion of matter meets the possibility of its localization. This point arises from the structure of the metric and the rules of relativistic velocity addition, not from speculation. Before the critical point K, matter exists in a diffuse state; afterward, the possibility of collapse or structure formation emerges. Thus, v=c=0 serves as a physical characteristic of extreme dynamics, explaining the transition from expansion to structure formation.

In the proposed geometry, the interpretation of the same physical state depends on the observer’s frame of reference. For example Figure 5, an observer at point O, analyzing events at point E, may describe the state v=c=0 as a result of matter reaching the limit speed c. At the same time, an observer at the mirror-symmetric point E (for example, in a strong gravitational field) sees this state as a merging of material objects. In this region, the temporal coordinate almost stops due to gravitational time dilation. From the perspective of this observer, the motion of material points gradually slows down, and their relative velocity during merging asymptotically approaches zero. This behavior is not an arbitrary hypothesis but logically follows from the combination of the proposed geometry with relativistic relations, including gravitational effects.

To validate the theoretical plausibility of the state $v=c=0$, the following conceptual approach is proposed:

- Cosmological observations — analysis of local fluctuations in galaxy velocities relative to a reference frame. Regions with anomalously low expansion rates and possible density asymmetries are expected, consistent with the mirror-symmetric geometry.
- High-energy particles — investigation of velocity distributions in cosmic rays or accelerators. The aim is to identify cases of “local particle freeze” ($v\to0$) in relativistic velocity addition.
- Gravitational effects — numerical simulations of gas-dust cloud collapse considering the mirror-symmetric metric, checking for accelerated transitions from diffuse states to localized dense objects.
- Numerical stability verification — reproducing calculations using different methods of velocity addition to confirm that the critical state $v=c=0$ is stable and independent of the method.

Thus, $v=c=0$ is not merely a mathematical paradox but a testable physical feature of matter dynamics in extreme cosmology, potentially observable both in cosmological surveys and in high-energy particle experiments.

21. Conclusion

The proposed geometry was developed to expand the possibilities for analyzing and visualizing physical processes related to gravity and relativistic effects. It demonstrates consistency with the classical Schwarzschild metric, while simultaneously providing new tools for interpreting and predicting states of matter, including matter ↔ antimatter transitions and critical phase states.

The main advantages of the model are its visual clarity, stability of preliminary calculations under extreme conditions, and its ability to simplify the analysis of complex systems, such as planetary, stellar, and galactic structures. At the same time, the geometry does not claim to replace classical methods but can serve as their extension, offering more illustrative and predictable results.

Of course, there are certain limitations. One of them is the behavior of matter at points O and E. In critical cases, we observe that the same event occurs at these different points with different interpretations, which is logically impossible. This suggests that these points are interconnected, and within the framework of such geometry, one might attempt to consider them as a single entity. However, this is already a topic for a separate study.

On the one hand, this geometry simplifies the visualization of processes in space, but at the same time it inevitably raises new questions.

By visualizing and perceiving such space, one can say that:

- It has a labyrinthine structure.
- Wherever the observer moves, they always feel at the center of space.
- Once inside, the observer becomes trapped and can never leave.

Our real space is likely far more complex than we are accustomed to thinking—it is just that our eyes perceive it in a familiar way.

It can also be said that the “moment before the instant of collision” is the moment when the absolute temperature of space approaches zero.

The limitations of the model are related to the need for further verification before applying it to real space.

Some predictions are partly theoretical in nature. The visualization of gravitational and relativistic effects is limited in completeness.

Scaling the model for complex systems requires additional refinements and computational approaches.

Overall, the proposed geometry opens new prospects for scientific research: it combines the stability and predictability of classical methods with the ability to analyze new states, which may make it a useful tool for future studies in gravitational physics, astrophysics, and related disciplines.

Conflict of Interest

The authors declare no conflict of interest.

Funding

This research received no external funding.

Data Availability Statement

No data were generated or analyzed in this study.

References

[1] Misner, Thorne, Wheeler, Gravitation, W. H. Freeman, 1973.

[2] Wald, R. M., General Relativity, University of Chicago Press, 1984.
[3] Hobson, E. et al., General Relativity: An Introduction for Physicists, Cambridge University Press, 2006, chap. on visualizing gravity.

[4] Luminet, J.-P., "Visualizing black holes," Scientific American, 1995.

[5] Schwarzschild, K., Sitzungsberichte der Königlich Preussischen Akademie der Wissenschaften, 1916.

[6] Carroll, S., Spacetime and Geometry: An Introduction to General Relativity, Addison-Wesley, 2003, ch. about black holes.

[7] Shapiro, S. L., Teukolsky, S. A., Black Holes, White Dwarfs, and Neutron Stars, Wiley, 1983.

[8] Rezzolla, L., & Zanotti, O., Relativistic Hydrodynamics, Oxford University Press, 2013.

[9] Luminet, J.-P., "Visualizing black holes," Scientific American, 1995 — for examples of visualization of relativistic effects.

[10] Frolov, V.P., Novikov, I.D., Black Hole Physics: Basic Concepts and New Developments, 1998.

[11] Hobson, E. et al., General Relativity: An Introduction for Physicists, 2006, ch. on visualizing gravity.

[12] Einstein, A. (1905). On the Electrodynamics of Moving Bodies. In: The Principle of Relativity, Dover Publications, 1952.
[13] Courant, R., Robbins, H., What is Mathematics?, Oxford University Press, 1996, Ch. 1 — for triangles inscribed in a circle.
[14] Schutz, B. F., A First Course in General Relativity, 2nd Edition, Cambridge University Press, 2009, Ch. 5 (derivation of the Schwarzschild radius and time dilation).

[15] Mikheili Mindiashvili, “A Geometric Interpretation of Lorentz Length Contraction Using an Inscribed Triangle in a Circle,” viXra:2506.0150, https://vixra.org/abs/2506.0150.

[16] Ashby N., Relativity in the Global Positioning System, Living Reviews in Relativity, 2003.

[17] Taylor E.F., Wheeler J.A., *Spacetime Physics*, 1992
[18] Rindler, W., Introduction to Special Relativity, 2nd Edition, Oxford University Press, 1991, Ch. 3
[19] Einstein, A. *Relativity: The Special and the General Theory*. Methuen & Co., 1920.

[20] Einstein, A., Zur Elektrodynamik bewegter Körper, 1905.

[21] French, Special Relativity, 1968.

[22] Rindler, W., Introduction to Special Relativity, 2006.
[23] Einstein, 1905; Rindler, 2006.
[24] Particle Data Group, Review of Particle Physics, 2022.

[25] Goldstein, Classical Mechanics, 3rd ed., 2002.

[26] Polchinski, String Theory, 1998.

[27] Greene, The Elegant Universe, 1999.
[28] Rindler, Introduction to Special Relativity, 2006.

[29] Williams et al., Lunar Laser Ranging Tests of the Equivalence Principle, 2004.
[30] Williams, J.G., Turyshev, S.G., Boggs, D.H. Lunar Laser Ranging Tests of the Equivalence Principle with the Earth and Moon. International Journal of Modern Physics D, 18(7), 1129–1175 (2009).
[31] Bethe, H., Quantum Mechanics of One- and Two-Electron Atoms, 1957.

[32] Sakurai, Modern Quantum Mechanics, 2017.
[33] Bethe & Salpeter, Quantum Mechanics of One- and Two-Electron Atoms, 1957.

[34] Greiner, Relativistic Quantum Mechanics, 2000.

[35] Hawking, S. W., Penrose, R. The Singularities of Gravitational Collapse and Cosmology, Proc. Roy. Soc. Lond. A, 1970.
[36] J. Meeus, Astronomical Algorithms, 2nd Edition, Willmann-Bell, 1998; NASA Planetary Fact Sheet, https://nssdc.gsfc.nasa.gov/planetary/factsheet/

[37] Born, M., & Wolf, E. Principles of Optics, 7th edition, Cambridge University Press, 1999.

[38] Hecht, E. Optics, 5th edition, Pearson, 2017.
[39] Saleh, B. E. A., & Teich, M. C. Fundamentals of Photonics, 3rd edition, Wiley, 2019.

[40] Yeh, P. Optical Waves in Layered Media, 2nd edition, Wiley, 2005.
[41] Heavens, O. S. Optical Properties of Thin Solid Films, Dover Publications, 1991

[42] Jenkins, F. A., & White, H. E. Fundamentals of Optics, 4th edition, McGraw-Hill, 2001.

[43] Collin, R.E. Foundations for Microwave Engineering. 2nd ed., Wiley, 2001.

[44] Pozar, D.M. Microwave Engineering. 4th ed., Wiley, 2012.

[45] Marcuvitz, N. Waveguide Handbook. McGraw-Hill, 1951.

[46] Senior, T.B.A. Electromagnetic Scattering. Academic Press, 1995.

[47] Balanis, C.A. Advanced Engineering Electromagnetics. 2nd ed., Wiley, 2012.

[48] Smart, W.M., Textbook on Spherical Astronomy, 1977.

[49] Born, M., Wolf, E., Principles of Optics, 1999.

[50] Hapke, B., Theory of Reflectance and Emittance Spectroscopy, 2012.

[51] Berry, M.V., Upstill, C., Catastrophe Optics, 1980.
[52] Hofmann-Wellenhof, B., Lichtenegger, H., GNSS – Global Navigation Satellite Systems, 2008.

[53] Snyder, J.P., Map Projections – A Working Manual, 1987.

[54] Thompson, L., Atmospheric Refraction Effects on Geodesy, 1995.
[55] Griffiths, D.J., Introduction to Quantum Mechanics, 2017.

[56] Goldstein, H., Classical Mechanics, 1980.

[57] Landau, L.D., Lifshitz, E.M., Quantum Mechanics, 1977.

[58] Abramowitz, M., Stegun, I.A., Handbook of Mathematical Functions, 1964.

[59] Bender, C.M., Orszag, S.A., Advanced Mathematical Methods for Scientists and Engineers, 1978.

[60] Olver, F.W.J., Asymptotics and Special Functions, 1974.

[61] Kahniashvili T.A., Machabeli G.Z. "Generation of the electrostatic field in the pulsar magnetosphere plasma", 1997. arXiv: astro-ph/9711266

[62] Chicone, C. & Mashhoon, B. "The generalized Jacobi equation", Class. Quantum Grav. 21, L139–L144 (2004). arXiv: gr-qc/0406118